4.1 INTRODUCTION

Pharmaceutical formulation development involves complex procedure which includes various process and formulation variables that can affect quality of final product. The effect of these individual parameters and their interaction can affect the quality of critical quality attribute.

Plackett Burman Design (PBD) is a 2-level experimental design which is used to screen large number of variables in fewer experimental runs. It is also known as screening design. It only includes main effects (1). In this design, each factor is presented at two levels, low level (-1) and high level (+1). The response is calculated using the regression equation 4.1:

$$Y = B_0 + B_1X_1 + B_2X_2 + B_3X_3 + \cdots + B_nX_n \ldots\ldots\ldots\ldots\ldots Equation\ 4.1$$

Response surface methodology (RSM) is the group of mathematical and statistical techniques which is used to elucidate functional relationship between a response of interest (dependent variables) and a number of input variables (independent variables). A Box-Wilson Central Composite Design (CCD) commonly called a central composite design,' contains an imbedded factorial or fractional factorial design with center points that is augmented with a group of 'star points' that allow estimation of curvature (1). The star point represents new extreme values (low and high) for each factor in the design. The response is calculated using the regression equation 4.2:

$$Y = B_0 + B_1X_1 + B_2X_2 + B_3X_3 + B_{11}X_{11}^2 + B_{22}X_{22}^2 + B_{33}X_{33}^2 + B_{12}X_1X_2 + B_{13}X_1X_3 + B_{23}X_2X_3 \ldots\ldots\ldots\ldots\ldots\ldots\ldots\ldots\ldots\ldots\ldots Equation\ 4.2$$

In this mathematical approach, each experimental response (Y) can be represented by a quadratic equation of the response surface. Y is the measured response and b is the estimated co-efficient for the factor X. The co-efficient corresponding to linear effects (X_1 and X_2), interaction (X_1X_2) and the quadratic effects (X_1^2 and X_2^2) were determined from the results of experiments (2).

Asenapine maleate loaded Solid Lipid Nanoparticles (AM-SLNs) were prepared using high speed homogenization followed by ultrasonication method. The formulation and process parameters were screened using Plackett Burman Design (PBD) and critical factors were further optimized by applying Central Composite Design (CCD), a type of RSM.

4.2 MATERIALS

Asenapine maleate (AM) was received as a gift sample from Alembic Pharmaceuticals Ltd., Vadodara, India. Glyceryl Monostearate (GMS) was purchased from Loba Chemie Pvt Ltd., Mumbai, India. Poloxamer 188 was purchased from Sigma Aldrich, Germany. D-α-Tocopheryl Polyethylene Glycol 1000 Succinate (TPGS) was obtained from Antares Health Products, Inc, USA. All other chemicals and reagents used were of analytical grade.

4.3 EQUIPMENT

Name of Equipment	**Manufacturer**
High speed homogenizer (HSH)	T-25 digital Ultra-Turrax, IKA® India Private Limited, India
Probe sonicatior	LABSONIC®M, Sartorius Ltd, Mumbai, India
Zeta sizer	Zeta sizer Nano series, Malvern Instruments, UK
Centrifuge CPR 30	Remi, India
VirTis Advantage Plus XL-70	SP Scientific, USA
Transmission Electron Microscope (TEM)	Philips, Tecnai 20, Holland
UV-VIS Spectrophotometer 1800	Shimadzu, Japan
Differential Scanning Calorimeter (DSC)	Shimadzu, Japan
Fourier Transform Infra-red spectrophotometer (FTIR)	FTIR, Shimadzu, Japan
X Ray Diffraction (XRD)	Philips, PW 1710, South Africa

4.4 SCREENING OF SOLID LIPID

Briefly, 500 mg of lipid was melted at a temperature 5°C above the melting point of lipid. Accurately weighed quantity of drug was added in increments and dissolved in molten lipid under stirring till drug was completely dissolved. The lipid-drug mixture was dissolved in organic solvents and amount of dissolved drug was determined by measuring absorbance using UV- spectroscopy (UV 1800, Shimadzu AS, Japan) at 270 nm (3).

4.5 PREPARATION OF SOLID LIPID NANOPARTICLES

SLNs were prepared by high speed homogenization followed by ultrasonication method as reported previously (4). Briefly, lipid was melted 5 °C above its melting point; AM was added to molten lipid and this lipid phase was dispersed in the aqueous surfactant solution at the same temperature of lipid using a homogenizer (T-25 digital Ultra-Turrax, IKA® India Private Limited, India). The obtained emulsion was ultrasonicated using a probe sonicator (Labsonic, Sartorius, Germany). The resulting dispersion was cooled in an ice bath to produce SLN.

4.6 EXPERIMENTAL DESIGN

4.6.1 Initial Risk Assessment: Ishikawa diagram

Ishikawa (fishbone) diagram was used to determine critical processing/formulation variables which can have an impact on the Critical Quality Attributes (CQAs) of AM-SLNs. Particle size (PS) and entrapment efficiency (EE) were selected as product Quality Attributes (QAs) (5).

4.6.2 Preliminary investigation of critical variables

After identifying the variables which can have influence on the product QAs from ishikawa diagrams, preliminary investigation of variables was carried out on the basis of risk priority. Preliminary optimization for selected process and formulation variables was carried out by changing one variable at a time while keeping the other constant. The influence of these variables on the particle size and entrapment efficiency were studied to determine lower and upper values for a screening design study.

4.6.3 Risk Analysis: Plackett Burman Design (PBD)

Initial screening of significant variables was carried out using PBD for their relative influence on the particle size and entrapment efficiency of the SLNs. The high and low values for each factor were selected on the basis of the results obtained from preliminary investigation. The PBD was constructed with 12 runs using Minitab version 16 (Minitab Inc., State College, PA, USA).

Key factors selected were X_1: Homogenization speed, X_2: Homogenization time, X_3: Sonication time, X_4: Sonication amplitude, X_5: Concentration of lipid, X_6: Concentration of surfactant, and X_7: Concentration of TPGS. The responses selected were particle size and entrapment efficiency.

4.6.4 Optimization using Central Composite Design (CCD): A Response Surface Methodology

A central composite design was used to optimize critical factors and to estimate main, interaction, and quadratic effects of the independent variables on CQA of AM loaded SLN. Based on the results obtained from PBD, three critical variables i.e. X_1: Lipid concentration, X_2: Surfactant concentration and X_3: Sonication time were taken as independent variables and particle size and entrapment efficiency were taken as dependent variables. Coded and actual values are shown in table 4.1.

Table 4.1: The coded and actual values of independent variables of AM-SLNs

Factors	Levels		
	-1	**0**	**+1**
X_1: Lipid Concentration (%)	2.5	5	7.5
X_2: Surfactant Concentration (%)	2	2.5	3
X_3: Sonication Time (min)	5	10	15

4.6.5 Response surface and contour plots

Contour plot is a graphic representation of the relationships between two variables in two dimensions. Contour plots and response surface plots are helpful to understand effect of two variables on response while keeping the third variable constant. Response surface plot aids in understanding of main and interaction effects of independent variables on responses (6). Contour and response surface plots were generated using Design expert 7 (Stat-Ease, Inc., USA).

4.6.6 Establishment of design space

The ICH Q8 defines design space as "the multidimensional combination and interaction of input variables and process parameters that have been demonstrated to provide assurance of quality". Design space was generated using Design expert software and constraints for the desired response (minimum particle size and maximum entrapment efficiency) were selected. The batch suggested by software was prepared using procedure as described above and predicted value was compared with experimental value.

4.6.7 Analysis of design space robustness

Analysis of design space was performed using design expert by plotting overlay plot with response higher and lower to the established design space. The software

suggested values for variables in and around established design space along with value of the desired responses.

4.6.8 Statistical analysis

The results were presented as mean ± standard error of the mean. The results were analyzed using the statistical software Minitab 16 and Design expert 7 (Stat-Ease, Inc., Minneapolis, USA). The experimental data were validated by Analysis of Variance (ANOVA), regression coefficient, and p value less than 0.05 was considered as significant.

4.7 LYOPHILIZATION OF SLNs AND OPTIMIZATION OF CRYOPROTECTANT

Freeze-drying has been considered as a good technique to improve the long-term stability of colloidal nanoparticles (7). Lyophilization, the most important drying process for biologicals, usually consists of three process steps. An aqueous solution is frozen, and subsequently, water is removed by sublimation during primary drying. Non-frozen water is removed by diffusion and desorption during secondary drying (8).

The optimized SLN formulation was lyophilized using lyophilizer (Virtis, SP Scientific, USA). Different cryoprotectants (Trehalose dihydrate, Mannitol and Sucrose) at different ratio (1:1 %w/w, 1:2 %w/w, 1:3 %w/w) were tried to select the appropriate cryoprotectant. SLN dispersion (2 ml) was taken in 10 ml semi-stoppered vials with rubber closures and frozen for 24 h at -80°C and then lyophilized for 24 h in the lyophilizer. Finally, the lyophilized samples were sealed under anhydrous conditions and stored until further characterization (9,10). Ratio of final particle size (after lyophilization, S_f) and initial particle size (before lyophilization, S_i) was calculated to finalize the cryoprotectant based on lowest S_f/S_i ratio.

4.8 CHARACTERIZATION

4.8.1 Determination of particle size

The particle size (PS) of the SLNs was determined by photon correlation spectroscopy using a Zetasizer (Malvern Instruments, Malvern, UK) (6). Each sample was diluted 10 times and particle size was measured using Zetasizer. Each measurement was carried out in triplicate.

4.8.2 Zeta potential measurement

The electrophoretic mobility (mm/s) was converted to zeta potential by in built software using Helmholtz–Smoluchowski equation. Each sample was diluted and zeta potential was measured using Zetasizer.

4.8.3 Determination of entrapment efficiency

The entrapment efficiency (%EE) was determined by measuring amount of unentrapped AM in SLN dispersion. SLN dispersion was centrifuged at 12000 rpm for 30 min so as to settle the SLN pellet. 1 ml of supernatant was dissolved in 10 ml of methanol, the solution was filtered and amount of free drug in the supernatant was determined by measuring absorbance at 270 nm in UV spectrophotometer (UV 1800, Shimadzu AS, Japan) (11). % EE was calculated from the following equation:

$$\%EE = \frac{\text{Total amount of drug added} - \text{free drug}}{\text{Total amount of drug added}} \times 100 \ldots\ldots\ldots\ldots\ldots\ldots\ldots\ldots \text{Equation 4.3}$$

4.8.4 Determination of total drug content

Drug content was determined by dissolving 1 ml of AM-SLNs dispersion in methanol. Suitable dilution was made and absorbance were measured at 270 nm using UV spectrophotometer to determine amount of AM present.

4.8.5 Differential Scanning Calorimetry (DSC)

The DSC thermograms of AM, GMS, physical mixture of AM and GMS and lyophilized AM-SLNs formulation were taken on a Differential Scanning Calorimeter (Shimadzu DSC-60) between 40 and 250 °C at a heating rate of 10 °C/min with Nitrogen supplied at 30 ml/min.

4.8.6 Fourier Transform Infra-red spectroscopy (FTIR)

The IR spectra of AM, GMS, physical mixture of AM and GMS and lyophilized AM-SLNs were recorded on Fourier Transform Infra-red spectrophotometer (Shimadzu, Japan).

4.8.7 X Ray Diffraction (XRD) study

The X-ray diffraction (XRD) studies of AM, GMS, physical mixture of AM and GMS and lyophilized AM-SLNs were carried out by wide angle X-Ray scattering (Philips, PW 1710) with a copper anode using Sc as detector.

4.8.8 Transmission Electron Microscopy (TEM)

For this study, 20 µl of SLN dispersion was taken on carbon filmcoated on copper grid and allowed to air dry. Then it was treated with phosphotungstic acid for negative staining. After 5min the grid was placed in the sample probe inserted in Transmission

Electron Microscope (Philips, Tecnai 20, Holland) and observed at 200 kV accelerating voltage.

4.9 IN VITRO DRUG RELEASE STUDY

The in vitro drug release from SLN formulation was carried out by the dialysis bag diffusion technique. The release profile of drug from SLN was compared with drug suspension.

Dialysis membrane having molecular weight cut off 12000-14000 Da was obtained from Himedia Laboratories Pvt. Ltd. The membrane was kept under running water for 3 h for removing glycerol followed by treatment of membrane with sodium sulphide solution (0.3% w/v) at 80°C for 1 minute to remove sulphur compounds. It was then washed with hot water (60°C) for 2 minutes, followed by acidification with a 0.2% (v/v) solution of sulphuric acid for 1 min, and subsequent rinsing with hot water to remove the acid. Then the dialysis membrane was dipped overnight in the diffusion medium before in-vitro release study for thorough wetting of the membrane.

The in vitro release studies of SLNs were carried out in gastric fluid (pH 1.2) and phosphate buffer pH 6.8. AM-SLNs dispersion and AM suspension equivalent to 10 mg was placed in the dialysis bag, clamped at both ends and introduced into a 50 mL of phosphate buffer. The entire system was kept under magnetic stirring at 100 rpm/min at 37±1°C and covered to prevent water evaporation. At predetermined time intervals, the aliquots were withdrawn and replaced with fresh diffusion medium. The samples were filtered and drug concentration was determined by a UV spectroscopy at 270 nm (12,13).

4.9.1 Drug release data modelling

The drug release data interpretation could be harmonized by means of mathematical equations, which fit the results under kinetic models. Furthermore, the application of these models allows the prediction of the drug release mechanism(s) from diverse pharmaceutical formulations (14).

There are number of kinetic models, which describe the release of drug from the dosage form. Because qualitative and quantitative changes in a formulation may alter drug release and may have influence on in vivo performance, developing tools that facilitate product development by reducing the necessity of bio-studies is always desirable. Hence. the use of in vitro drug dissolution data to predict in vivo bio-

performance can be considered as the rational development of controlled release formulations (14,15).

The kinetic analysis of the release data was done by fitting to different exponential equations such as Zero order, First order, Higuchi, and Korsmeyer Peppas to characterize the release. These models (14,15) were fitted to the data obtained from drug release study, in order to select the model that best described the release profile from SLNs (Table 4.2).

Table 4.2: Various release kinetic models

Model	Equation
Zero order	$Q_0 - Q_t = K_0 t$
First order	$\log C = \log C_0 - {kt}/{2.303}$
Higuchi	$f_t = Q = k_H t^{1/2}$
Hixson Crowell	$W_0^{1/3} - W_t^{\frac{1}{3}} = \kappa t$
Korsmeyer-Peppas	${M_t}/{M_\infty} = Kt^n$

where Q_t is the amount of drug dissolved in time t, Q_0 is the initial amount of drug and K_0 is the zero-order release constant, C_0 is the initial concentration of drug, k is the first order rate constant, Q is the amount of drug released in time t, K_H is the Higuchi dissolution constant, W_0 is the initial amount of drug, W_t is the remaining amount of drug at time t and κ (kappa) is a constant incorporating the surface volume relation. M_t is the drug released at time t, M_∞ is the quantity of drug released at infinite time, K is the kinetic constant, and n is an exponent to characterize different release mechanisms.

4.10 EX VIVO PERMEATION STUDY

Ex vivo permeability studies of SLNs and Drug suspension were performed to determine transport of drug through biological membrane. The studies were carried out using rat stomach and intestine. The protocol was approved by the Institutional Animal Ethics Committee of M.S. University of Baroda, Vadodara, India (MSU/IAEC/2017-18/1643). Rats (250-300g) were sacrificed by euthanasia and a part of stomach and intestine was immediately removed, thoroughly washed and placed in phosphate buffer pH 7.4. A volume equivalent to 10 mg AM each of SLN and drug suspension were added in lumen of stomach and tied at each end with a thread. Then the tissue was placed in an organ tube containing 30 ml of phosphate buffer pH 7.4

with continuous aeration, the temperature was maintained 37±0.5 °C. At predetermined time intervals (0.5, 1 and 2 h), samples were withdrawn and replenished by the same volume of fresh buffer solution. After 2 h, the contents of stomach were transferred into the lumen of intestine and tied at each end with a thread. At predetermined intervals of time (4, 6, 8, 10, 12 and 24 h), aliquots were withdrawn from the receptor compartment, filtered through 0.22µ membrane filter and analyzed by UV spectrophotometer (UV 1800, Shimadzu AS, Japan) at 270 nm (16,17).

4.11 STABILITY STUDY

The stability study was carried out to determine the effect of formulation additives on the stability of drug and to determine the physical stability of the prepared formulation under conditions of storage temperature and Relative Humidity (RH). The stability of SLNs was carried out for 3 months at 2-8 °C and Room temperature (30±2°C/60% ± 5% RH). The sample was withdrawn after a period of 0, 1, 2 and 3 months and the effect on particle size, zeta potential and drug content was determined (18).

4.12 RESULTS AND DISCUSSION

4.12.1 Screening of solid lipid

The maximum solubility of AM was obtained in Glyceryl monostearate (GMS) (Figure 4.1). So, GMS was selected as a lipid phase for formulation development.

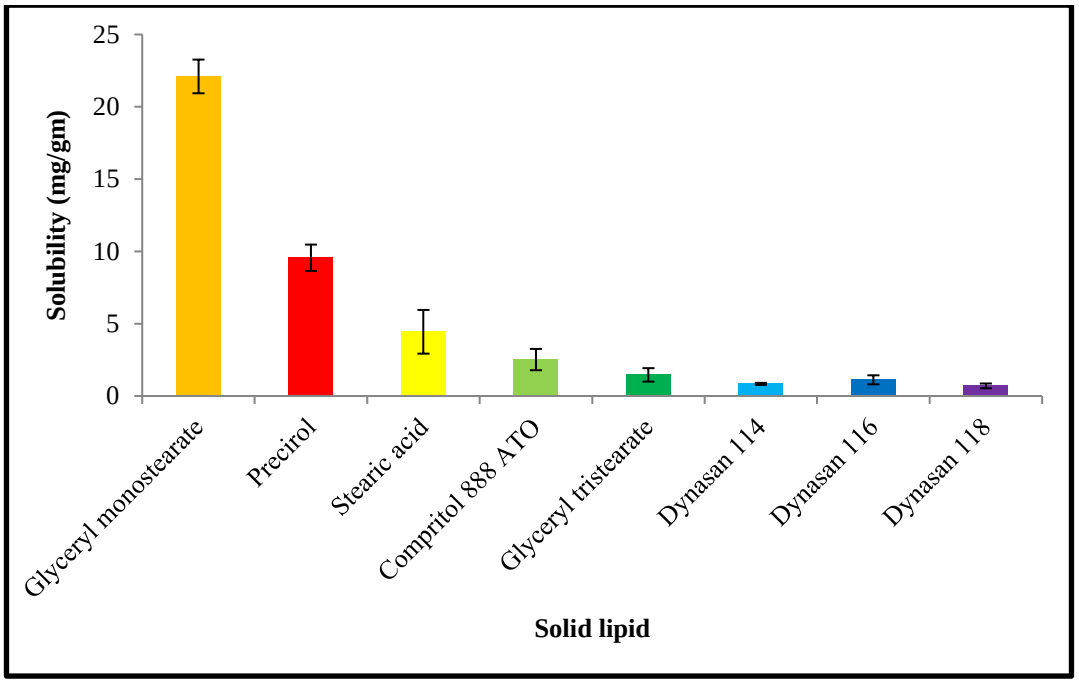

Figure 4.1: Solubility of Asenapine maleate in various lipids

4.12.2 Risk identification: Ishikawa diagram

Ishikawa diagram was generated for factors affecting QAs of SLNs and these factors were divided in three categories viz., Process, formulation and environment. Critical factors that were identified amongst all were studied to evaluate their effect on QAs. Ishikawa diagram for particle size and entrapment efficiency are shown in figure 4.2(a) and 4.2(b) respectively.

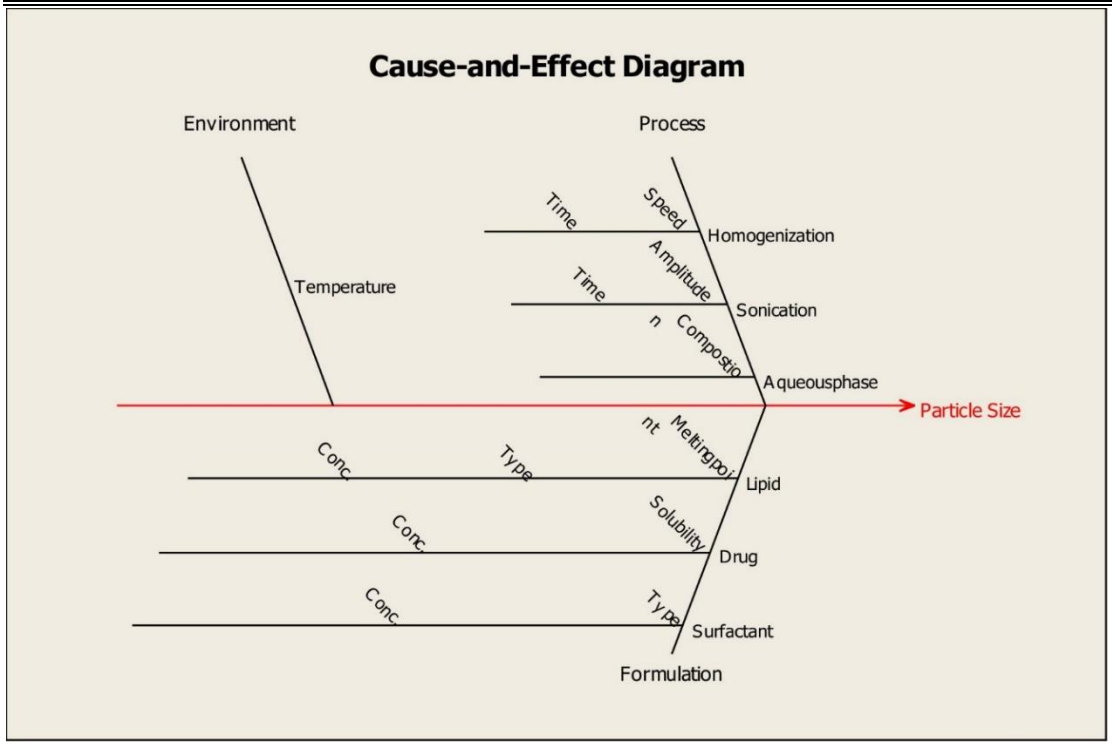

(a)

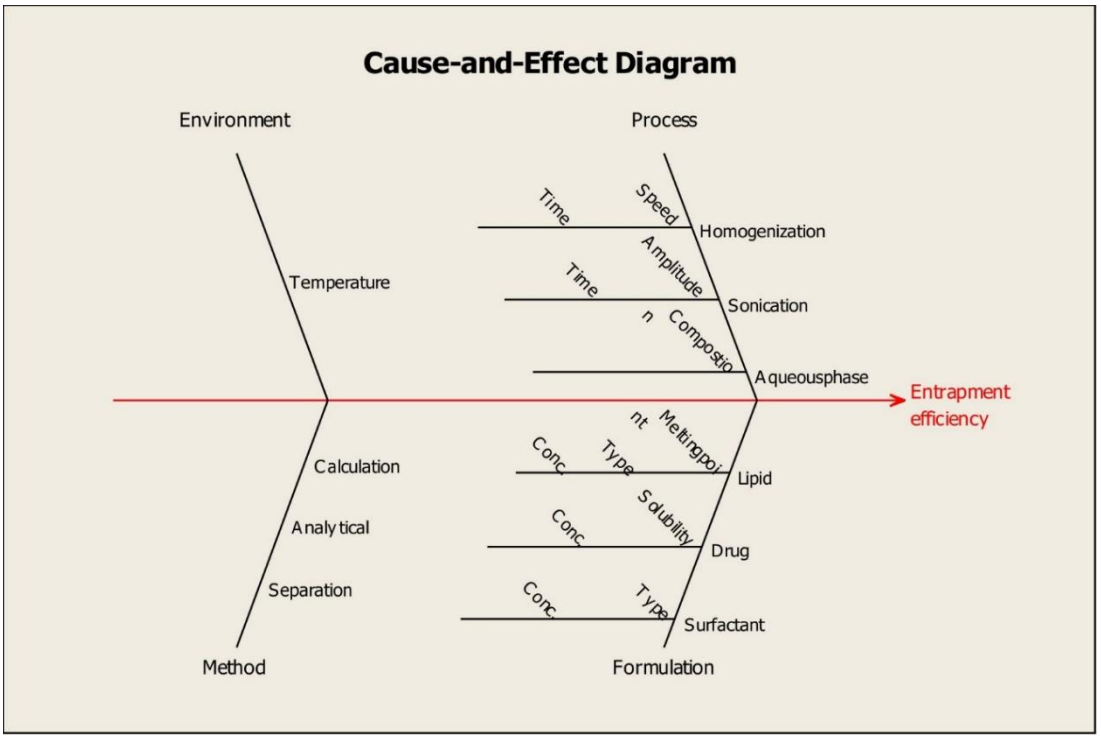

(b)

Figure 4.2: Ishikawa diagram for (a) Particle size and (b) Entrapment efficiency of AM-SLNs

4.12.3 Preliminary investigation of variables

4.12.3.1 Influence of process variables

4.12.3.1.1 Influence of homogenization speed

It was observed that homogenization speed had major effect on particle size as compared to entrapment efficiency (Table 4.3). As the homogenization speed was increased from 8000 to 10000 rpm, the particle size was decreased. However, further increase in homogenization speed from 10000 to 16000 increased the particle size. This might be because at higher homogenization speed higher shear rate was generated which led to increase in viscosity of continuous phase. Shearing mechanisms predominate when viscosities increase, leading to larger particle sizes (19). Moreover, at higher homogenization speed the flow behavior changed from Newtonian to shear thickening which could lead to formation of aggregates. Entrapment efficiency was found to be slightly lower at 8000 rpm. With further increase in homogenization speed from 8000 to 16000 rpm, EE was found to be increased.

Table 4.3: Effect of homogenization speed on particle size and entrapment efficiency of AM-SLNs

Homogenization Speed (rpm)	Particle size (nm)	Entrapment efficiency (%)
8000	251.2±3.1	67.34±3.58
10000	149.7±2.7	77.40±4.40
12000	197.9±4.8	78.00±2.06
14000	213.8±3.2	78.91±2.86
16000	277.5±2.5	79.20±3.18

4.12.3.1.2 Influence of homogenization time

The high speed accompanied by time is very important factor for the preparation of SLN. It was observed that homogenization time had significant effect on particle size (Table 4.4). As homogenization time was increased from 1 min to 10 min, the particle size was gradually decreased from 607.2 nm to 120.3 nm. With further increase to 15 min, particle size increased from 120.3 nm to 279.0 nm as longer homogenization time may cause instability of colloidal particles due to high input of energy that leads to aggregation of colloidal particles into larger particles (19,20). It was observed that entrapment efficiency was gradually increased with homogenization time. This could

be because shorter period of homogenization (1 and 2.5 min) may fail to produce nanoparticles and hence lower EE. As homogenization time increased from 2.5 to 10 min, appropriate shear rate is provided to lipid dispersion which will lead to formation of stable colloidal particles with increased entrapment efficiency. Further increase in homogenization time decreased entrapment efficiency due to aggregation of particles. Hence, medium duration of homogenization is advantageous (20).

Table 4.4: Effect of homogenization time on particle size and entrapment efficiency of AM-SLNs

Homogenization time (min)	Particle size (nm)	Entrapment efficiency (%)
1	607.2±6.7	68.38±3.58
2.5	320.3±7.5	69.56±4.12
5	218.4±5.2	72.55±2.51
10	120.3±4.1	76.96±3.40
15	279.0±6.5	74.38±2.82

4.12.3.1.3 Influence of sonication time

Ultrasonication with the aid of ultrasonic probes has been used as a catalyst for chemical reaction formation, in disrupting biological membranes, and for the preparation of different types of nanoparticles. During the fabrication of nanoparticles, ultrasonic probes generate high-frequency mechanical vibrations in which small vacuum cavities are formed. These cavities then rapidly implode to create microscopic shock waves. This process, known as cavitation, is extremely powerful when the collective energy of all the imploding cavities is combined. The tremendous energy released within the liquid by sonication, however, can produce considerable heat, which may impact the process ability of high-melting point lipids and subsequently the formation of SLNs (21,22).

Sonication time had major effect on particle size and was the critical step in particle size reduction. It was observed that (Table 4.5) as sonication time was increased from 1 min to 12.5 min, the particle size was gradually decreased which might be attributed to energy provided by sonication which reduced the size of coarse dispersion into nano-droplets (22). Entrapment efficiency was not significantly affected by sonication time up to 10 min. But at 12.5 min sonication time, entrapment efficiency was found to be decreased from to 62.34% which was attributed to breakdown of particles causing loss of drug and reduced entrapment efficiency with higher sonication time.

Table 4.5: Effect of sonication time on particle size and entrapment efficiency of AM-SLNs

Sonication time (min)	Particle size (nm)	Entrapment efficiency (%)
1	341.0±6.9	77.92±3.80
2.5	261.3±3.2	79.23±4.45
5	236.7±2.6	78.34±2.36
7.5	213.0±4.7	74.34±3.51
10	147.4±6.8	77.91±5.20
12.5	108.3±3.5	62.34±1.89

4.12.3.1.4 Influence of sonication amplitude

Sonication amplitude has direct correlation with sonication intensity. At low amplitude setting, low intensity of sonication will be delivered. Sonication works by producing cavitation transit in the dispersion and its effectiveness depends on viscosity and density of dispersion which in turn is affected by formulation temperature. It is essential to maintain temperature above melting point of lipid to facilitate breakdown of dispersion (22). The results showed that at 20 to 40% sonication amplitude, particle size was more than 200 nm indicating that low intensity of sonication was unable to reduce particle size efficiently. When sonication amplitude was increased from 40 to 60%, particle size was reduced to 127 nm (Table 4.6). Further increase in sonication amplitude didn't affect particle size. Entrapment efficiency was found to be decreased from 78% to 73% with increase in sonication amplitude from 20 to 80%. This could be due to increase in sonication amplitude decreased particle size which ultimately led to loss of drug and entrapment efficiency was reduced. At high sonication amplitude, high-frequency mechanical vibrations were generated which led to loss of drug and hence, EE was decreased.

Table 4.6: Effect of Sonication amplitude on particle size and entrapment efficiency of AM-SLNs

Sonication amplitude	Particle size (nm)	Entrapment efficiency (%)
20	261.2±5.5	78.70±2.87
40	208.7±8.4	76.14±1.58
60	127.3±4.6	75.63±3.45
80	125.4±3.9	73.04±4.78

4.12.3.2 Influence of formulation variables

4.12.3.2.1 Influence of lipid concentration

Lipid concentration was the major influencing factor on both particle size and entrapment efficiency. As the lipid concentration was increased from 1 to 10%, particle size increased from 69.6 nm to 242.3 nm (Table 4.7). As the lipid amount is increased, the viscosity of lipid melt increases, ultimately affecting the shearing efficiency of homogenizer during the initial phase of emulsification. This also increased collision of particles and led to increase in particle size (23). Another reason might be that the sonication energy is less efficiently distributed in viscous dispersion as compared to less viscous dispersion. As lipid concentration was increased, the entrapment efficiency was found to be increased from 18 to 95%. This was expected because at higher lipid concentration, viscosity of lipid phase will be increased which will result into faster solidification which in turn will prevent drug diffusion from inner phase to aqueous phase (24). Moreover, more amount of lipid will be available for drug loading so EE was increased.

Table 4.7: Effect of lipid concentration on particle size and entrapment efficiency of AM-SLNs

Lipid concentration (%)	Particle size (nm)	Entrapment efficiency (%)
1	69.6±3.5	18.83±5.77
2.5	122.3±5.1	46.52±7.03
5	150.7±6.7	84.96±6.34
7.5	207.6±8.4	89.47±4.55
10	242.3±4.8	95.45±3.19

4.12.3.2.2 Influence of surfactant concentration

The amount of surfactant plays important role in nanoparticle formation. It was observed that as surfactant concentration was increased from 0.5% to 5%, particle size was gradually decreased from 347.5 nm to 133.5 nm (Table 4.8). At lower surfactant concentration, the amount of surfactant available is not able to cover the nano-droplets which will lead to their coalescence which in turn increases the particle size. At higher surfactant concentration, more amount of surfactant will be available to reduce interfacial tension between two phases, enable the lipid to become efficiently emulsified in the aqueous phase, and stabilize the nano-droplets and prevent their

coalescence (25). As surfactant concentration increased from 0.5% to 2.5%, entrapment efficiency was found to be increased. Further increase in surfactant concentration from 2.5% to 5% reduced entrapment efficiency. With increase in the concentration of surfactant in external phase, drug may diffuse out from lipid nanodroplets and solubilize in the micelles in aqueous phase, leading to reduced entrapment efficiency (23).

Table 4.8: Effect of surfactant concentration on particle size and entrapment efficiency of AM-SLNs

Surfactant concentration (%)	Particle size (nm)	Entrapment efficiency (%)
0.5	347.5±3.7	46.35±3.92
1	251.3±2.3	56.54±4.11
2	217.9±4.9	66.19±5.34
2.5	145.1±4.1	77.41±4.32
5	133.5±2.8	62.49±6.73

4.12.3.2.3 Type of lipid

Two different lipids GMS and Precirol were studied. GMS produced smaller particle size as compared to Precirol. The possible explanation might be the longer chain length of Precirol (C_{37}) as compared to GMS (C_{21}) and its higher molecular weight which makes it bulkier and less susceptible to packaging into small particle size and produces larger particles (24). Entrapment efficiency was found to be higher with GMS because solubility of drug in Precirol was less as compared to GMS (Table 4.9).

Table 4.9: Effect of type of lipid on particle size and entrapment efficiency of AM-SLNs

Type of lipid	Particle size (nm)	Entrapment efficiency (%)
GMS	133.9±3.6	75.46±5.31
Precirol	224.9±3.1	52.23±4.29

4.12.3.2.4 Type of surfactant

It was observed that combination of surfactants efficiently reduced particle size as compared to single surfactant. Among 6 types of surfactants, it was observed that Poloxamer:TPGS produced smallest particle size. Particle size increased as follows: Cremophor EL>Tween 80>Poloxamer 188> Tween 80: Poloxamer 188> Tween

80:TPGS>Poloxamer 188: TPGS (Table 4.10). This might be because combination of surfactants helps in reducing interfacial tension more efficiently and helps in stabilization of nano-droplets (26,27).

Entrapment efficiency of batches prepared using different surfactants increased as follows:

Poloxamer 188: TPGS> Tween 80:TPGS> Tween 80> Poloxamer 188> Cremophor EL> Tween 80: Poloxamer 188

It is also reported that combination of ionic and non-ionic stabilizers is preferred for emulsification technology; therefore, combination of ionic and non-ionic surfactants may provide SLNs with special properties due to their steric and electostatic effects (27). Hence, combination of Poloxamer and TPGS was selected as surfactant.

Table 4.10: Effect of type of surfactant on particle size and entrapment efficiency of AM-SLNs

Type of surfactant	Particle size (nm)	Entrapment efficiency (%)
Poloxamer 188	307.9±6.9	68.03±3.72
Cremophor EL	498.1±5.5	67.97±3.29
Tween 80	394.2±3.6	70.78±5.62
Poloxamer 188: TPGS	145.5±4.9	80.32±2.76
Tween 80:TPGS	237.5±4.5	73.23±3.89
Tween 80: Poloxamer 188	292.3±3.7	62.34±4.33

4.12.3.2.5 Concentration of TPGS

It was observed that as the TPGS concentration increased, particle size was gradually decreased. This might be due to higher concentration of TPGS could help in stabilizing nanodroplets. The entrapment efficiency was increased upto 0.02% concentration of TPGS. Further increase in TPGS concentration from 0.03% to 0.05% decreased entrapment efficiency. The Critical Micelle Concentration (CMC) of TPGS is 0.025% w/v (26). Therefore, with increase in concentration of TPGS from 0.02% to 0.04%, drug may get diffused out from nanodroplets and solubilize drug in micelles leading to reduced entrapment efficiency.

Table 4.11: Effect of TPGS concentration on particle size and entrapment efficiency of AM-SLNs

TPGS concentration (%)	Particle size (nm)	Entrapment efficiency (%)
0.01	121.2±4.3	73.21±1.93
0.02	117.4±2.7	80.91±4.27
0.03	110.2±2.4	68.93±3.51
0.04	105.3±3.9	57.98±3.92
0.05	104.3±4.0	51.23±4.90

From the results of preliminary optimization, following range of variables were selected for screening design PBD (Table 4.12).

Table 4.12: Values of variables selected for PBD after preliminary optimization of AM-SLNs

PARAMETERS	VALUE	
	-1	+1
Homogenization Speed (rpm)	10000	14000
Homogenization time (min)	5	15
Sonication time (min)	2.5	15
Sonication amplitude (%)	40	80
Lipid concentration (%)	2.5	10
Surfactant concentration (%)	1	3
Concentration of TPGS (%)	0.01	0.03

4.12.4 SCREENING DESIGN: PLACKETT BURMAN DESIGN (PBD)

PBD aids in the beginning of formulation development to segregate various factors for their influence on major characteristics of formulation. PBD allows identifying critical factors with less number of runs (12 runs) but it doesn't include interaction effects of factors. The results of PBD are shown in table 4.13.

Table 4.13: PBD experimental runs of AM-SLNs

HS* (rpm)	HT* (min)	ST* (min)	SA* (%)	LC (%)	SC * (%)	TPGS conc. (%)	PS (nm)	EE (%)
14000	5	2.5	40	10	3	0.03	301.2±2.3	74.45±3.20
14000	15	2.5	80	2.5	1	0.01	255.1±1.7	61.02±2.56
14000	5	15	80	2.5	3	0.01	104.7±2.1	44.10±1.94
10000	15	2.5	40	2.5	3	0.03	197.2±1.2	57.02±2.30
14000	5	15	40	2.5	1	0.03	207.2±1.9	54.91±3.76
14000	15	15	40	10	3	0.01	264.2±2.5	61.01±1.50
10000	15	15	80	2.5	3	0.03	151.1±1.1	56.10±2.20
10000	5	2.5	40	2.5	1	0.01	325.6±2.8	65.34±3.52
10000	15	15	40	10	1	0.01	298.7±3.2	72.87±2.77
10000	5	2.5	80	10	3	0.01	397.0±1.4	67.13±3.82
14000	15	2.5	80	10	1	0.03	468.4±1.9	81.02±2.15
10000	5	15	80	10	1	0.03	372.4±2.9	75.23±1.90

*Abbreviations: HS: Homogenization speed, HT: Homogenization time, ST: Sonication time, SA: Sonication amplitude, LC: Lipid concentration, SC: Surfactant concentration. *Data are presented as mean±SD, n=3.

4.12.4.1 Influence on Particle size

Seven high risk factors were identified in a risk analysis study to have potential impact on SLN particle size. As shown in table 4.14 for PS, most significant factors were lipid concentration, surfactant concentration and sonication time ($p<0.05$) relative to other factors. The magnitude of coefficients indicates its effect on response. A positive effect value indicates an effect that favors the response, and a negative value represents an inverse relationship between the response and the factor (5). So, lipid concentration had positive and surfactant concentration and sonication time had negative influence on PS. Further analysis using ANOVA indicated a significant effect ($p=0.032$) of all three (lipid concentration, surfactant concentration and sonication time) variables on the response ($p < 0.05$).

Table 4.14: Estimated effects and coefficients for particle size (coded units) of AM-SLNs

Term	Coef	Std error Coef	T	P
Constant	343.5	103.1	3.33	0.029
Homogenization speed	-0.005883	0.006509	-0.90	0.417
Homogenization time	-1.223	2.603	-0.47	0.663
Sonication time	-7.283	2.083	-3.50	0.025
Sonication amplitude	0.6442	0.6509	0.99	0.378
Lipid conc.	19.133	3.471	5.51	0.005
Surfactant conc.	-42.67	13.02	-3.28	0.031
Conc. of TPGS	435	1302	0.33	0.755

Main effects plot for particle size (Figure 4.3) indicted that PS was highly influenced by lipid concentration, surfactant concentration and sonication time whereas other factors had negligible effect on PS.

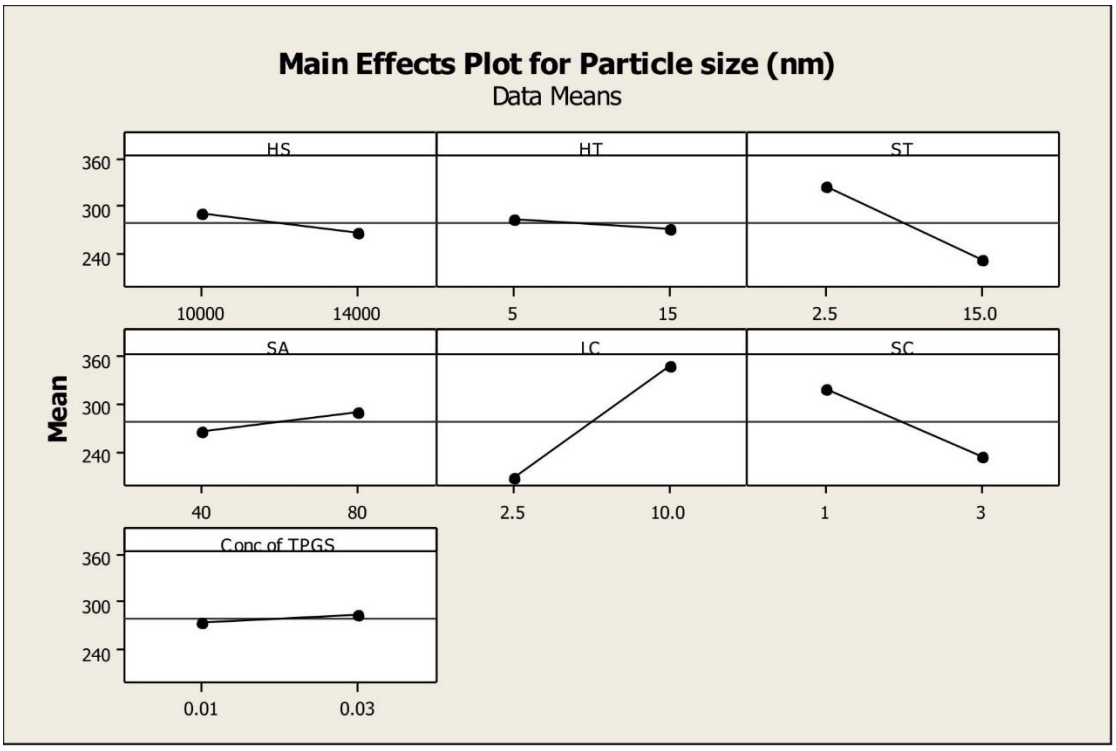

Figure 4.3: Main effect plot for Particle size of AM-SLNs

Pareto chart helps to prioritize main affecting variables amongst all selected variables. The effects are plotted in decreasing order of the absolute value of the effects. It indicates that any effects that extend beyond the reference line are considered as significant. Here, the chart (Figure 4.4a) shows that sonication time, lipid concentration and surfactant concentration are beyond the reference line and were considered as critical variables for particle size. Half normal plot displays the absolute value of each factor. Points that are away from the zero usually indicate significant effects (Figure 4.4b). Normal plot indicated that lipid concentration had positive whereas surfactant concentration, sonication time had negative effect on particle size (Figure 4.4c). This result is in accordance with effect analysis.

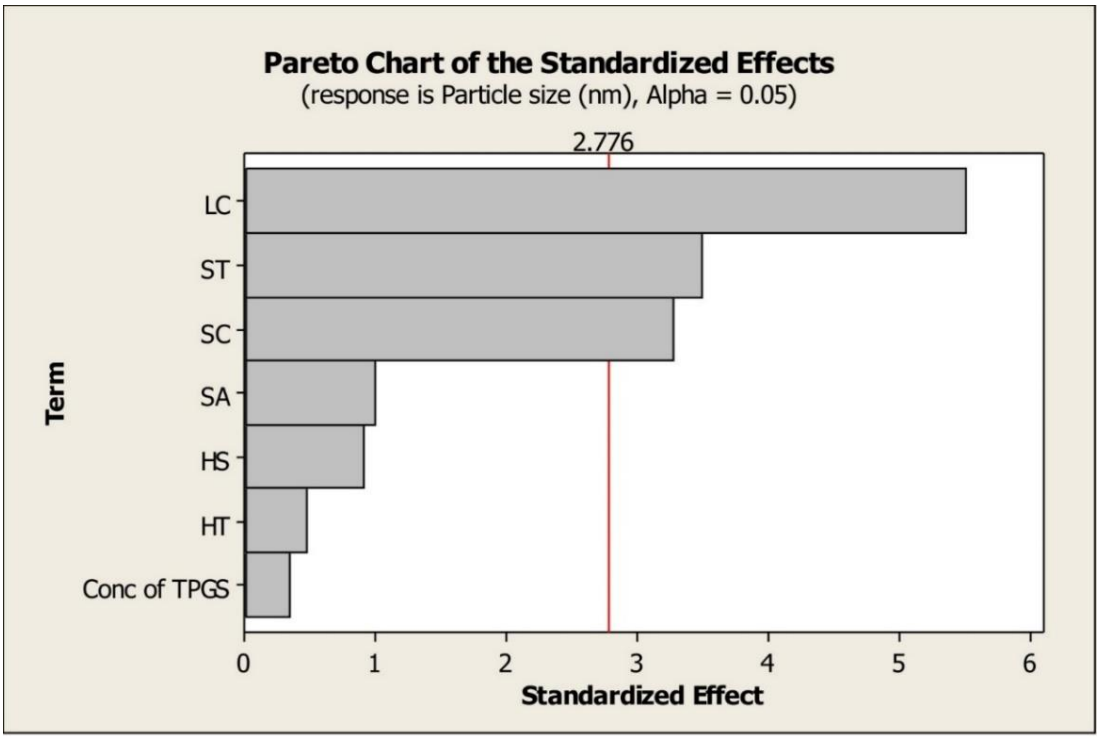

(a)

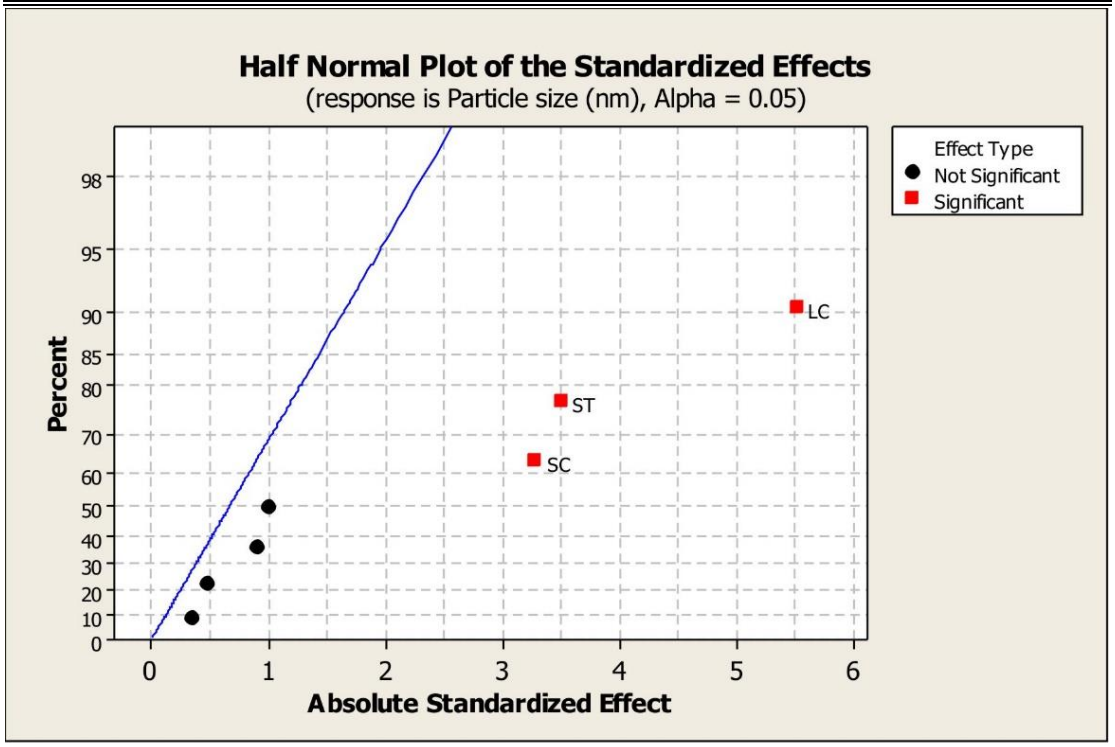

(b)

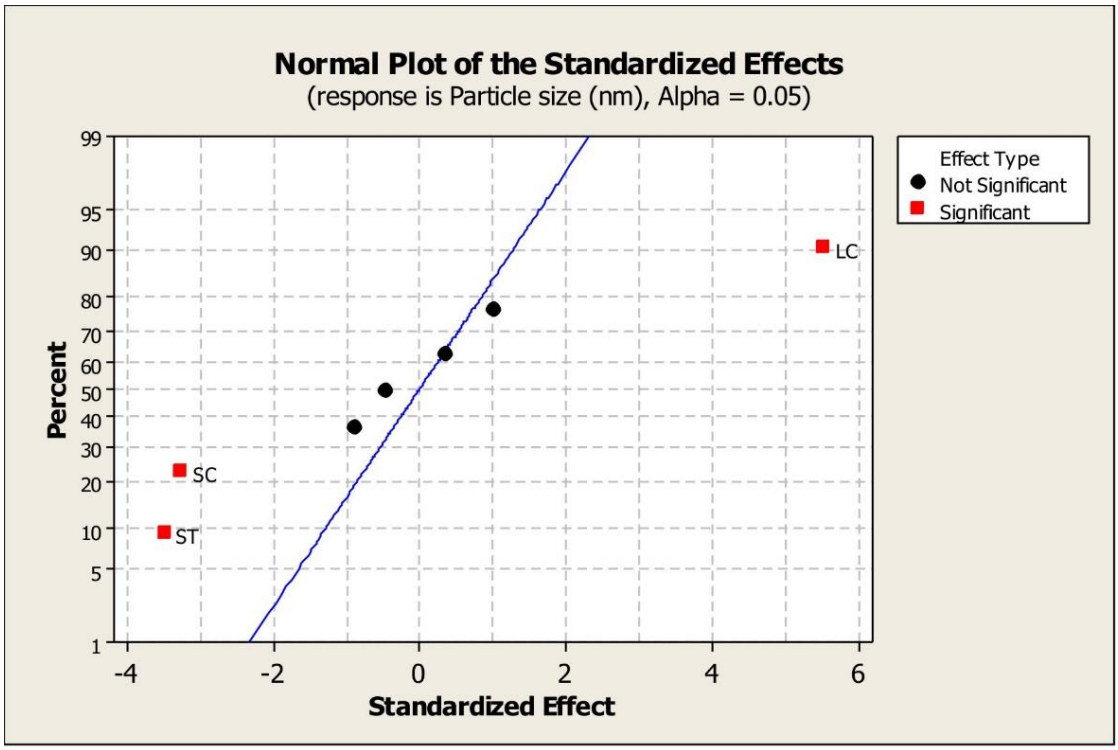

(c)

Figure 4.4: (a) Pareto chart (b) Half normal plot and (c) Normal plot for particle size of AM-SLNs

4.12.4.2 Influence on Entrapment efficiency (EE)

As shown in table 4.15 for EE, most significant factors were lipid concentration, surfactant concentration and sonication time ($p<0.05$). Further analysis using ANOVA also indicated a significant effect ($p=0.011$) of all three (lipid concentration, surfactant concentration and sonication time) on EE.

Table 4.15: Estimated effects and coefficients for entrapment efficiency (coded units) of AM-SLNs

Term	Coef	Std error Coef	T	P
Constant	67.521	7.920	8.53	0.001
Homogenization speed	-0.0007158	0.0004999	-1.43	0.225
Homogenization time	0.1313	0.2000	0.66	0.547
Sonication time	-0.5568	0.1600	-3.48	0.025
Sonication amplitude	-0.00417	0.04999	-0.08	0.938
Lipid conc.	2.0716	0.2666	7.77	0.001
Surfactant conc.	-4.2150	0.9999	-4.22	0.014
Conc. of TPGS	227.17	99.99	2.27	0.086

Main effect plot for EE (Figure 4.5) also indicted that it was highly influenced by lipid concentration, surfactant concentration and sonication time whereas other factors had negligible effect on EE.

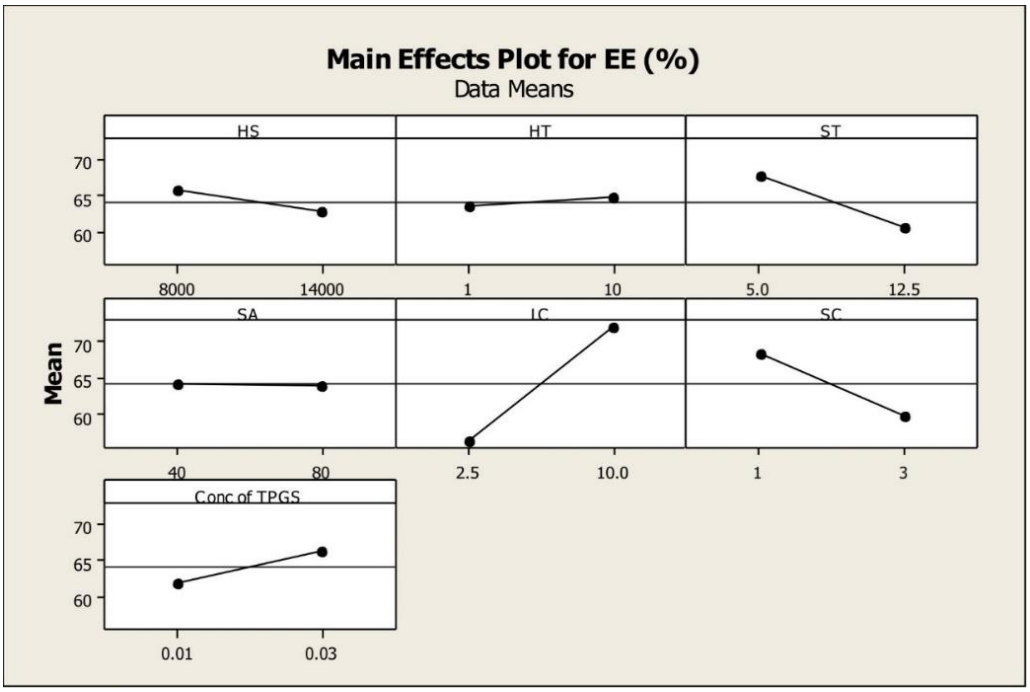

Figure 4.5: Main effect plot for entrapment efficiency of AM-SLNs

Pareto chart indicates (Figure 4.6a) that sonication time, lipid concentration and surfactant concentration are beyond the reference line and were considered as critical variables for entrapment efficiency. Normal plot indicated that lipid concentration had positive effect whereas sonication time and surfactant concentration had negative effect on entrapment efficiency (Figure 4.6c).

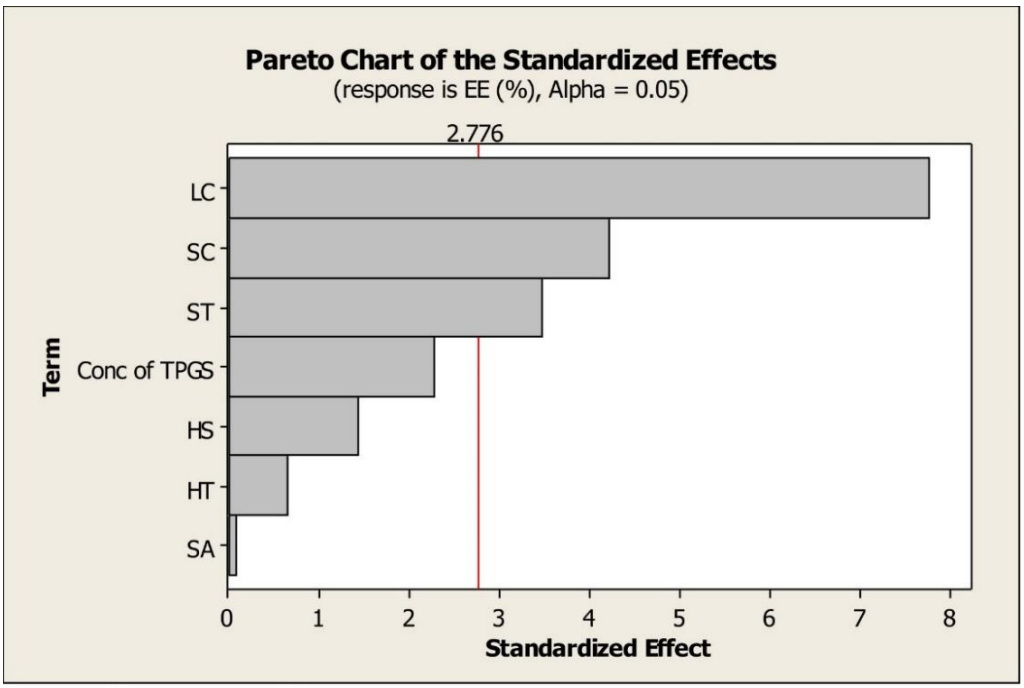

(a)

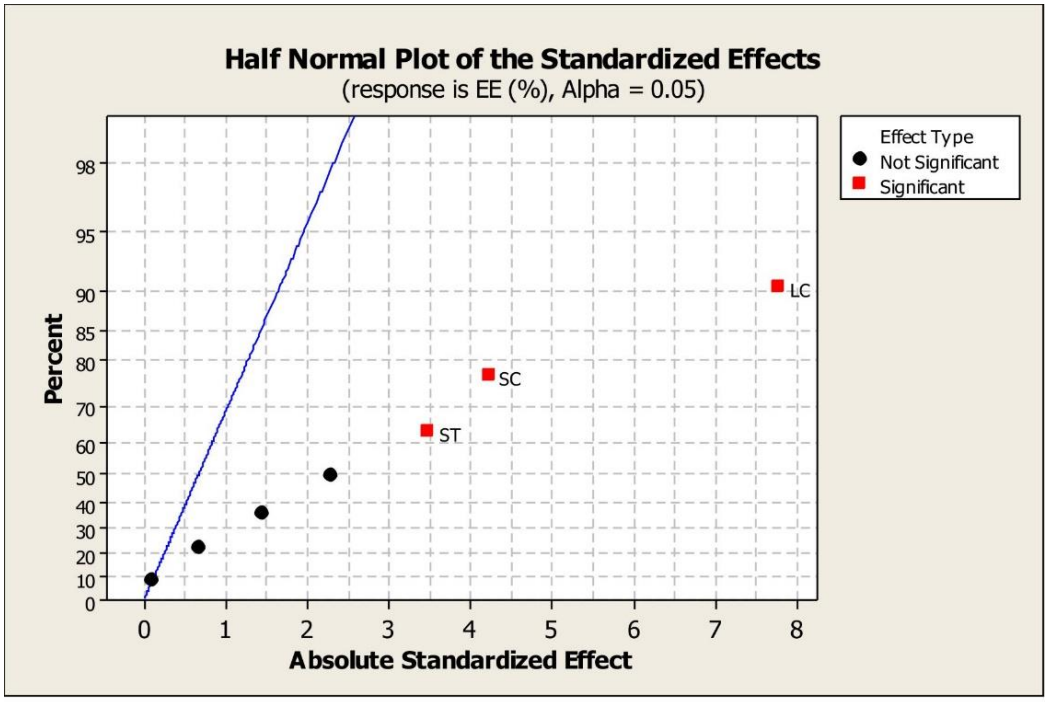

(b)

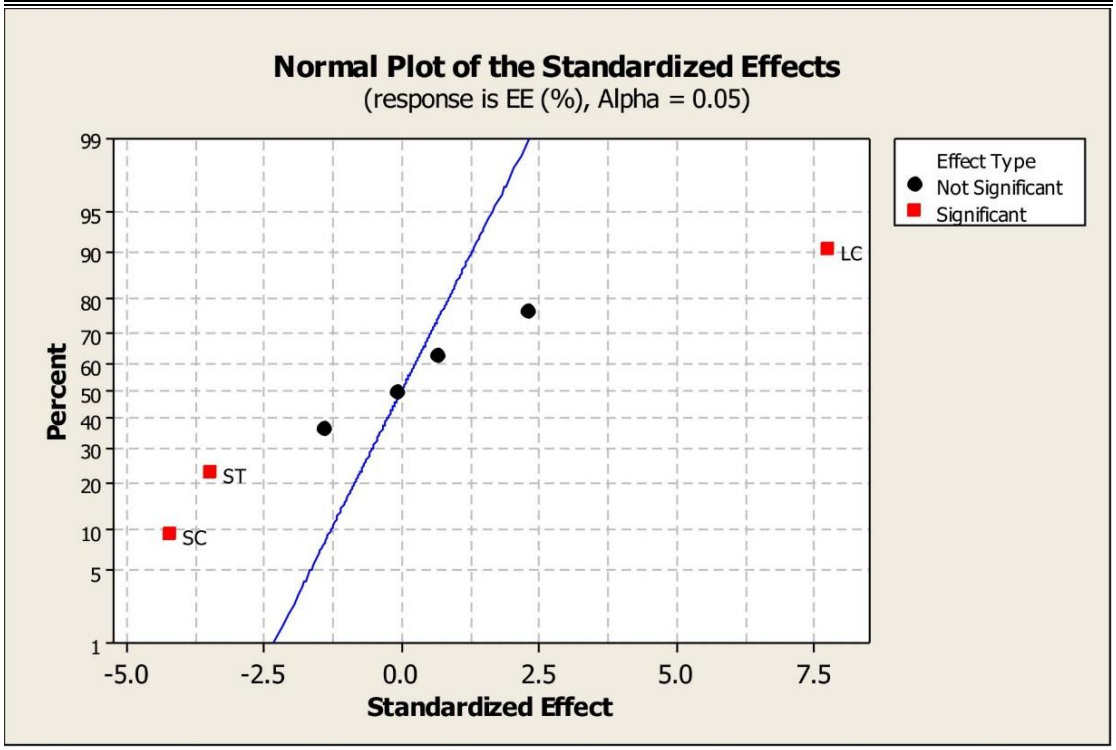

(c)

Figure 4.6 : (a) Pareto chart (b) Half normal plot and (c) Normal plot for entrapment efficiency of AM-SLNs

4.12.5 Optimization using CCD

Following the screening study, the three most significant factors (lipid concentration, surfactant concentration and sonication time) were optimized using CCD and results obtained from the experiments for CCD runs are shown in table 4.16.

Table 4.16: Central composite design experimental runs of AM-SLNs

Sr. No.	X_1 (%)	X_2 (%)	X_3 (min)	Y_1 (nm)	Y2 (%)
1	5	2.5	18.41	303.7±2.3	57.32±3.92
2	2.5	3	15	264.7±4.2	65.51±4.57
3	2.5	2	15	209.3±1.9	59.39±2.81
4	5	1.66	10	227.4±3.2	54.32±2.43
5	5	3.34	10	196.9±4.0	49.21±3.49
6	7.5	3	15	240.1±2.7	63.37±3.74
7	9.20	2.5	10	387.2±1.5	74.53±5.11
8	7.5	2	5	444.9±2.2	76.29±4.49
9	5	2.5	10	114.3±2.1	83.61±3.12
10	5	2.5	1.59	410.3±2.5	77.37±4.30
11	2.5	2	5	191.2±2.0	55.23±2.20
12	7.5	2	15	317.2±3.2	70.92±3.45
13	7.5	3	5	391.9±1.7	61.23±3.30
14	5	2.5	10	121.8±1.2	88.12±2.70
15	2.5	3	5	190.7±2.4	51.03±4.89
16	5	2.5	10	120.4±3.4	86.45±3.57
17	0.795518	2.5	10	135.9±1.6	40.17±2.88

4.12.5.1 Influence of independent variables on particle size

The following full model (Equation 4.4) polynomial equations were generated by the statistical analysis of the results.

$$Y_1 = +119.17 + 70.36X_1 - 9.26X_2 - 26.85X_3 - 23.12X_1X_2 - 46.45X_1X_3 + 3.97X_2X_3 + 49.30X_1^2 + 31.83X_2^2 + 83.04X_3^2 \ldots\ldots\ldots\ldots\ldots\ldots\ldots\ldots Equation\ 4.4$$

The regression coefficients having p value <0.05 were considered as significant factors. The terms having coefficients with p value>0.05 were least contributing in the prediction of response. Thus, neglecting non-significant (p>0.05) terms from the full model and applying regression between significant terms gave equation of reduced model (Equation 4.5) (20).

$$Y_1 = 119.17 + 70.36X_1 - 9.26X_2 - 26.85X_3 - 23.12X_1X_2 - 46.45X_1X_3 + 49.30X_1^2 + 31.83X_2^2 + 83.04X_3^2 \ldots\ldots\ldots\ldots\ldots\ldots\ldots\ldots Equation\ 4.5$$

Table 4.17: Effect tests analysis of independent variables on particle size of AM-SLNs

Source	Sum of Squares	df	Mean square	F Value	p-value prob>F
Model	185632.4194	9	20625.82437	108.6057217	< 0.0001
X_1	67599.9753	1	67599.9753	355.9491234	< 0.0001
X_2	1171.639099	1	1171.639099	6.169290865	0.0420
X_3	9845.135011	1	9845.135011	51.83977007	0.0002
X_1X_2	4278.125	1	4278.125	22.52655917	0.0021
X_1X_3	17260.82	1	17260.82	90.88721882	< 0.0001
X_2X_3	126.405	1	126.405	0.665588245	0.4415
X_1^2	27394.38775	1	27394.38775	144.2457377	< 0.0001
X_2^2	11421.27716	1	11421.27716	60.13898046	0.0001
X_3^2	77740.59604	1	77740.59604	409.3447799	< 0.0001
Residual	1329.402985	7	189.9147122		
Lack of Fit	1297.596318	5	259.5192637	16.31854519	0.0587
Pure Error	31.80666667	2	15.90333333		
Cor Total	186961.8224	16			

Based on the p value (Table 4.17), all factors were found to be significant ($p<0.05$) except X_2X_3. A positive value of X_1 in polynomial equations corresponds to an effect that favors the optimization, while a negative value of X_2 and X_3 corresponds to an inverse relationship on the particle size. The reason behind this effect was discussed in section 4.9.3.1 and 4.9.3.2.

The relationship between independent variables and dependent variables were elucidated using contour and response surface plots. It was observed that increase in X_1 increased particle size but no significant change in particle size was observed with change in X_2 which was in accordance with results obtained from effect analysis (Figure 4.7). It can also be seen that increase in X_3 decreased particle size which is also in accordance with effect analysis. As the sonication time increased, particle size was decreased upto 10 min. Increase in sonication time from 10 min to 15 min, increased particle size (Figure 4.8). It was reported that sonication efficiency

increases when the medium temperature is low. When the temperature of the medium increases due to cavitation, the medium expands, leading to the production of less energetic shock waves from bubble implosion (22). So, at higher sonication time, efficiency of sonication decreased which increased particle size. No prominent effect was observed on particle size while changing X_2 (Figure 4.9).

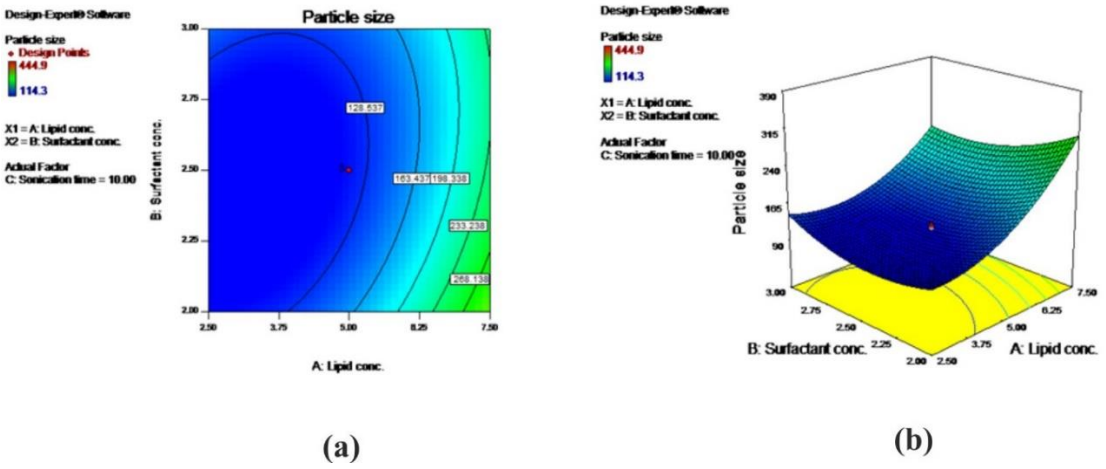

Figure 4.7 : (a) Contour and (b) Response surface plot showing effect of lipid concentration and surfactant concentration on particle size of AM-SLNs

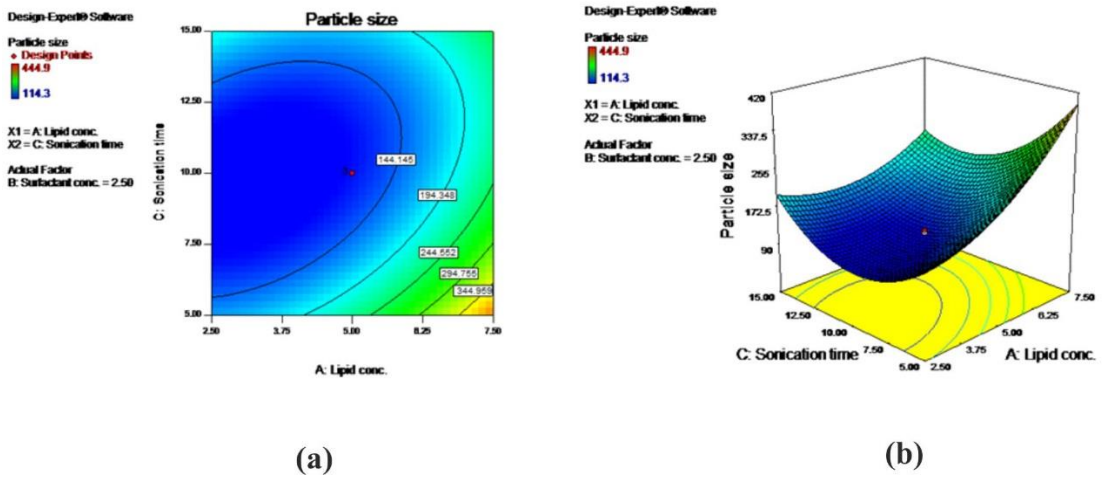

Figure 4.8: (a) Contour and (b) Response surface plot showing effect of lipid concentration and sonication time on particle size of AM-SLNs

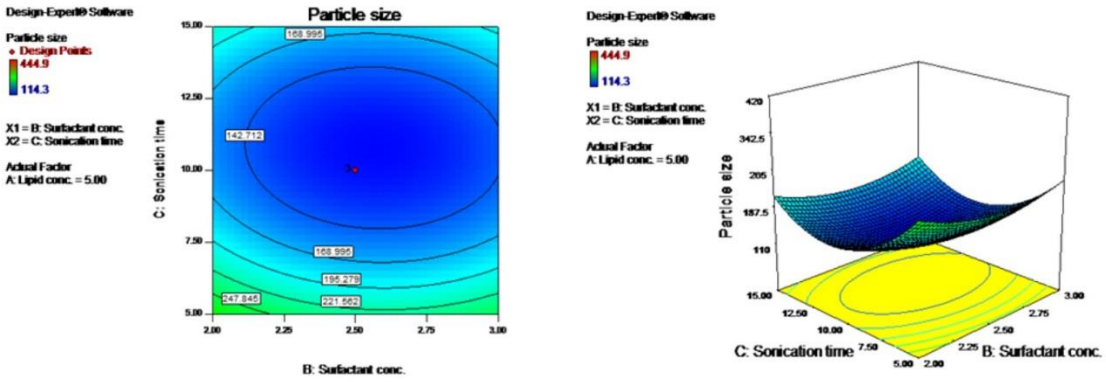

(a) **(b)**

Figure 4.9: (a) Contour and (b) Response surface plot showing effect of surfactant concentration and sonication time on particle size of AM-SLNs

4.12.5.2 Influence of independent variables on entrapment efficiency

The following full model (Equation 4.6) and reduced model (Equation 4.7) polynomial equations were generated by the statistical analysis of the results:

$$Y_2 = 85.69 + 7.21X_1 - 2.14X_2 - 1.34X_3 - 3.07X_1X_2 - 2.73X_1X_3 + 2.23X_2X_3 - 8.88X_1^2 - 10.86X_2^2 - 5.35X_3^2 \ldots\ldots\ldots\ldots\ldots\ldots\ldots\ldots Equation\ 4.6$$

Reduced model equation:

$$Y_2 = +78.85 + 7.21X_1 - 2.14X_2 - 7.30X_1^2 - 9.28X_2^2 \ldots\ldots\ldots\ldots\ldots\ldots\ldots\ldots Equation\ 4.7$$

Table 4.18: Effect tests analysis of independent variables on entrapment efficiency of AM-SLNs

Source	Sum of Squares	df	Mean square	F Value	p-value prob>F
Model	2708.259843	9	300.9177603	5.108564463	0.0214
X_1	709.5136987	1	709.5136987	12.04513972	0.0104
X_2	62.79267374	1	62.79267374	1.066006942	0.3362
X_3	24.54841544	1	24.54841544	0.416748957	0.5391
X_1X_2	75.2151125	1	75.2151125	1.276897882	0.2957
X_1X_3	59.7871125	1	59.7871125	1.014982691	0.3473
X_2X_3	39.7386125	1	39.7386125	0.674627059	0.4385
X_1^2	889.8160182	1	889.8160182	15.10606248	0.0060
X_2^2	1329.307392	1	1329.307392	22.5671376	0.0021
X_3^2	322.735622	1	322.735622	5.478957865	0.0518
Residual	412.3319452	7	58.9045636		
Lack of Fit	401.9337452	5	80.38674904	15.46166626	0.0619
Pure Error	10.3982	2	5.1991		
Cor Total	3120.591788	16			

Based on the p value (Table 4.18), X_1, X_1^2 and X_2^2 factors were found to be most significant ($p<0.05$) as compared to other factors. As seen in equation, X_1 had positive effect i.e. increase in X_1 increased the value of entrapment efficiency. X_2 had negative effect on the entrapment efficiency i.e. increase in X_2 reduced the entrapment efficiency.

The effect of independent factors on response variable entrapment efficiency was elucidated using contour and response surface plots. It was observed that increase in X_1 increased entrapment efficiency while increase in X_2 reduced entrapment efficiency which is in accordance with results obtained from effect analysis (Figure 4.10). At lowest X_1 and highest X_2 entrapment efficiency was decreased so it proved that interaction between these factors affected entrapment efficiency. Amongst factors X_1 and X_3, it was observed that slight change in entrapment efficiency was observed with X_3 (Figure 4.11). Response surface plot also indicated that X_2 had profound effect on entrapment efficiency (Figure 4.12).

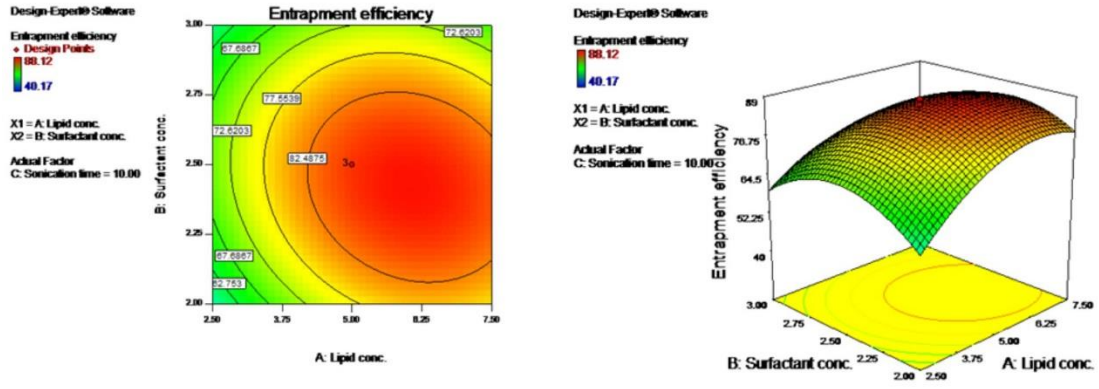

(a) **(b)**

Figure 4.10: (a) Contour and (b) Response surface plot showing effect of lipid concentration and surfactant concentration on entrapment efficiency of AM-SLNs

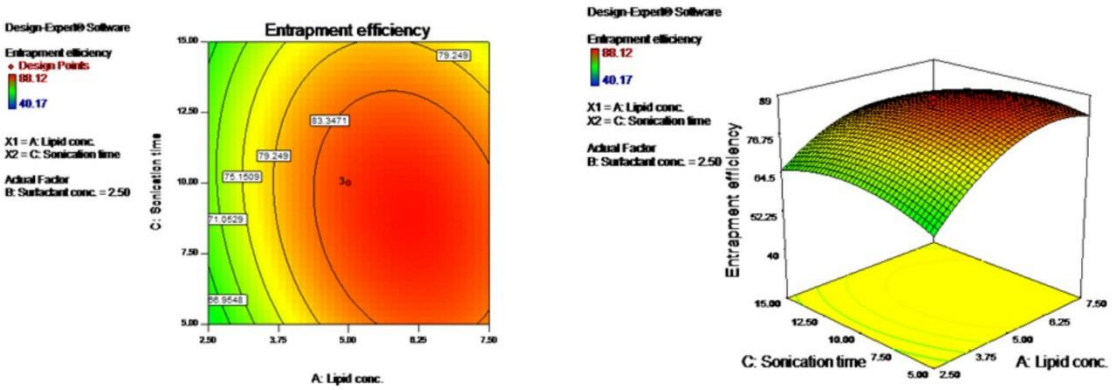

(a) **(b)**

Figure 4.11: (a) Contour and (b) Response surface plot showing effect of lipid concentration and sonication time on entrapment efficiency of AM-SLNs

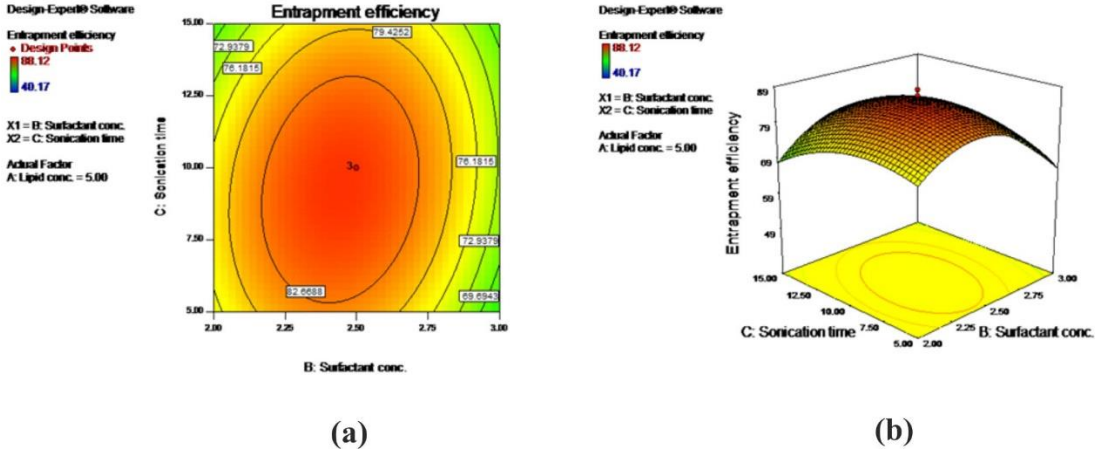

Figure 4.12: (a) Contour and (b) Response surface plot showing effect of surfactant concentration and sonication time on entrapment efficiency of AM-SLNs

4.12.5.3 Statistical analysis of designed experiment

The adequacy of the quadratic model was verified by ANOVA, lack of fit and multiple correlation coefficient (R^2) tests provided by Design- Expert software. The results of ANOVA showed that p value for response PS and EE was found to be <0.0001 (highly significant) and 0.0214 respectively, for quadratic model. Thus it can be concluded that all the responses fitted the model well ($p<0.05$) Moreover, the lack of fit test is another good statistical parameter for checking the fitness of the model. It compares the residual error with the pure error from the replicated design points. A model with a significant lack-of-fit (Prob>F value 0.10) lacks prediction efficiency, so a non-significant lack of- fit value in the model is highly desirable. The lack of fit value for PS and EE was found to be 0.0587 and 0.0619 respectively. All of these responses fitted in the cubic model showed a non-significant lack-of-fit ($p>0.1$), proving the adequacy of the model fit. Furthermore, the multiple regression analysis for the quadratic model is shown as R^2 value, which signifies the measure of the amount of variation around the mean explained by the model. In our study, the R^2 values for the responses PS and EE were 0.9929 and 0.8679 respectively.

4.12.5.4 Establishment of design space

Design space is the space within which the quality of the product can be built. The constraints for the responses were selected and predicted value was compared with experimental value. The observed value of particle size and entrapment efficiency were found to be in good aggreement with predicted values (Table 4.19).

Table 4.19: Predicted and experimental value of optimized batch of AM-SLNs suggested by software

Independent variable	**Value**	
Lipid concentration (%)	4.92	
Surfactant concentration (%)	2.49	
Sonication time (min)	10.13	
Response	**Predicted**	**Experimental**
Y_1 (nm)	112.8	114.3±5.4
Y_2 (%)	85.10	84.10±3.70

Desirability plot was generated using design expert software and its value was found to be 0.969 (Figure 4.13), which is near to 1 which indicates accuracy and suitability of predicted desirability for responses.

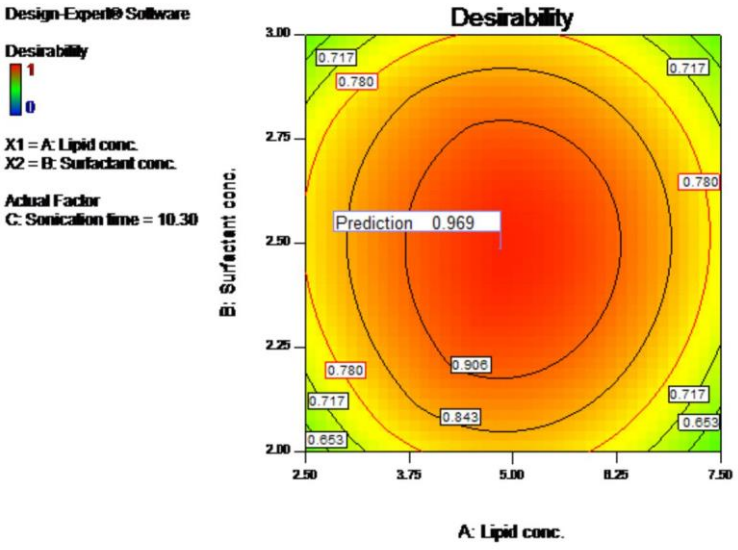

Figure 4.13: Desirability plot for optimized batch of AM-SLNs

4.12.5.5 Analysis of design space robustness

Analysis of design space is necessary for scale up point of view. The upper and lower ranges of the desired response were selected. Contour plots show how response variables (particle size and entrapment efficiency) relate to two continuous design variables (lipid concentration and surfactant concentration) while holding the third variable (sonication time) at 10.30 min. The yellow area inside each plot shows the range of lipid concentration and surfactant concentration where the criteria for both response variables are satisfied (Figure 4.14).

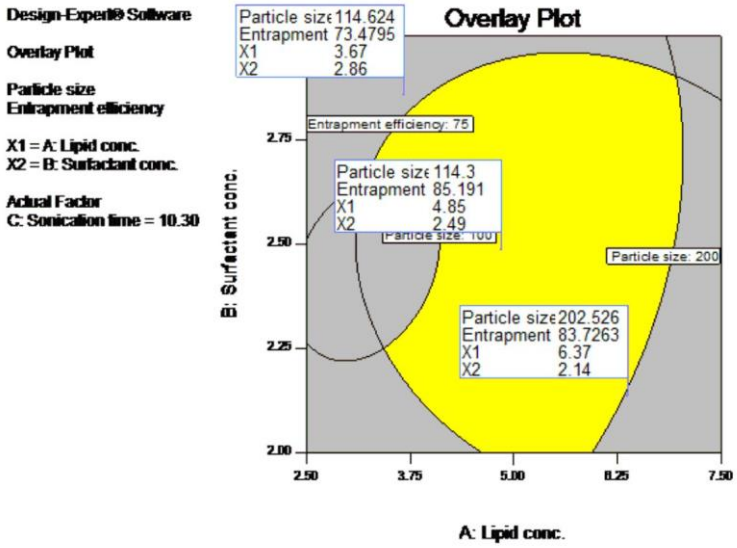

Figure 4.14: Overlay plot showing robustness of design space of AM-SLNs

It was observed (Table 4.20) that value of independent variables outside the design space showed variation in response so it proved that the design space was sensitive to variation in independent variables. The area selected inside the circle showed desired response proving the robustness of design space.

Table 4.20: Evaluation of sensitivity of obtained design space of AM-SLNs

X_1 (%)	X_2 (%)	X_3 (min)	Y_1 (nm)		Y_2 (%)	
			Predicted	**Observed**	**Predicted**	**Observed**
3.67	2.86	10.30	114.62	110.4±3.2	73.47	71.62±3.54
4.85	2.49	10.30	114.3	112.7±5.8	85.19	85.03±4.21
6.37	2.14	10.30	202.53	209.3±2.9	83.72	84.93±2.91

4.13 CHARACTERIZATION

4.13.1 Determination of particle size

The particle size of optimized batch was found to be 114.3±3.5 nm (Figure 4.15). Polydispersity index (PDI) is the measure of homogeneity of dispersion and usually ranges from 0 to 1. Value close to zero indicates a homogenous dispersion. The PDI value of optimized batch was found to be 0.188±0.010 indicating a narrow particle size distribution. The smaller particle size will provide large surface area, consequently providing high concentration of AM for absorption and thus, can improve its oral performance (28). Moreover, these SLNs with particle size below 200 nm will also promote lymphatic uptake (29).

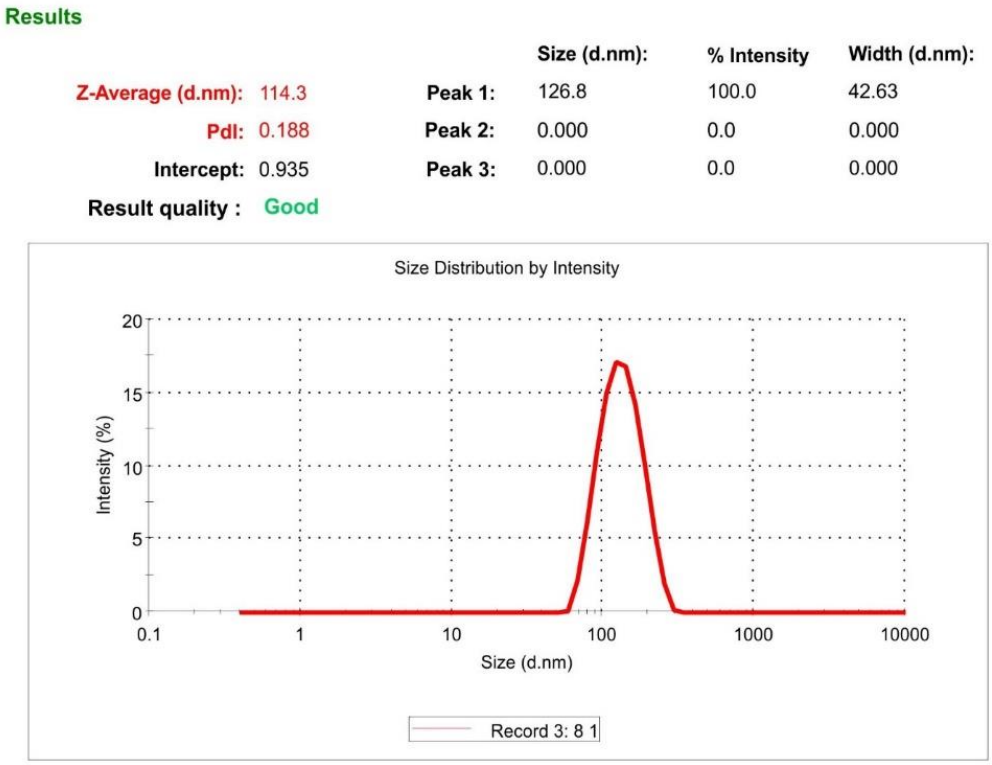

Figure 4.15: Particle size of optimized batch of AM-SLNs

4.13.2 Zeta potential determination

Zeta potential analysis indicates particle surface charge, and is considered predictive of formulation stability, particularly for emulsions and colloidal dispersions. The zeta potential of optimized batch was found to be -12.9±3.8 mV (Figure 4.16). The negative zeta value might be due to the presence of TPGS as surfactant in formulation. An overall net negative zeta potential of the lipid particles will lead to electric repulsion between the particles reducing the likelihood of their aggregation.

Results

		Mean (mV)	Area (%)	Width (mV)
Zeta Potential (mV): -12.9	Peak 1:	-9.84	66.6	4.68
Zeta Deviation (mV): 6.82	Peak 2:	-20.3	33.4	3.26
Conductivity (mS/cm): 0.546	Peak 3:	0.00	0.0	0.00

Result quality : See result quality report

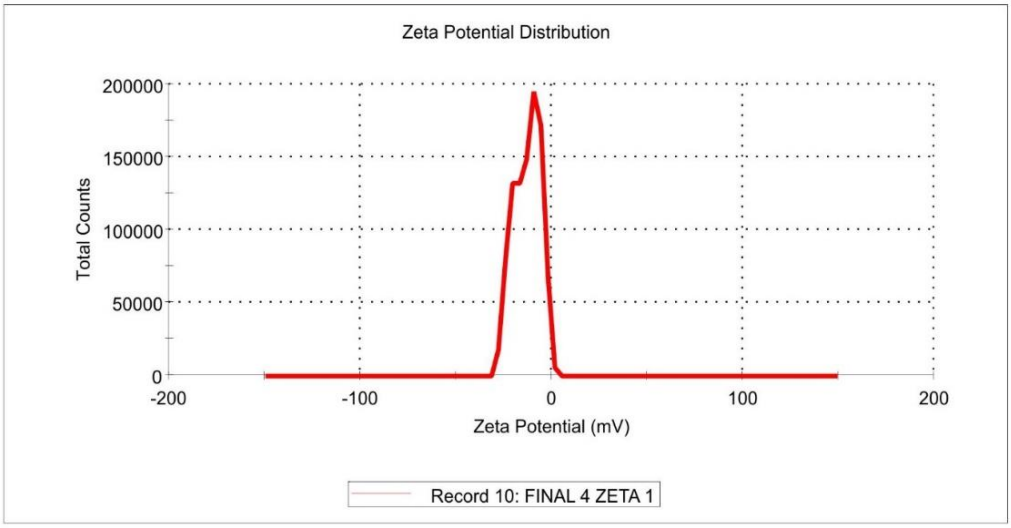

Figure 4.16:Zeta potential of optimized batch of AM-SLNs

4.13.3 Determination of entrapment efficiency and drug content

In this method of preparation, drug was completely dissolved in molten lipid at temperature above the melting point of lipid and there was no drug leakage or precipitation of drug during the preparation. Moreover, long chain fatty acids attached to the glyceride resulted in increased accommodation of lipophilic drug (30). Hence, the %EE of optimized batch was found to be 84.10±2.90% indicating drug was completely solubilized in GMS. The total drug content of optimized batch was found to be 99.1±1.2%.

4.13.4 Lyophilization of SLN and optimization of cryoprotectant

Cryoprotectants help in SLN stability by decreasing osmotic activity of water and crystallization (particle isolation hypothesis) and favoring the formation of glassy state of the frozen sample (amorphous glass theory). They prevent direct contact between lipid particles and they also interact with the polar groups of the surfactants and serve as a pseudo hydration shell (31-33). SLNs were lyophilized using different cryoprotectants in different ratios with respect to total solid content to find out optimum concentration of cryoprotectant. Cryoprotectant was selected on the basis of minimum enhancement ratio. It was observed that minimum enhancement ratio (1.16)

was observed with trehalose in the ratio of 1:3 with respect to solid content as compared to other cryoprotectants (Table 4.21).

Table 4.21: Optimization of cryoprotectants of AM-SLNs

Cryoprotectant	Ratio	Particle size (nm)*	PDI*	Enhancement ratio*
Initial	-	114.3±3.5	0.188±0.030	-
Trehalose	1:1	233.7±3.7	0.264±0.078	2.04
	1:2	178.7±4.3	0.453±0.120	1.56
	1:3	133.0±2.8	0.317±0.056	1.16
Sucrose	1:1	441.2±3.9	0.289±0.092	3.86
	1:2	382.3±2.7	0.410±0.034	3.34
	1:3	256.8±3.4	0.308±0.023	2.25
Mannitol	1:1	303.8±4.9	0.317±0.077	2.66
	1:2	443.1±2.9	0.567±0.129	3.88
	1:3	689.3±3.1	0.402±0.145	6.03

*Data are presented as mean±SD, n=3.

4.13.7 Fourier Transform Infrared Spectroscopy (FTIR)

FTIR spectra of AM, GMS, physical mixture of AM and GMS and lyophilized AM-SLNs are shown in figure 4.17. The FTIR spectra of AM showed characteristic peaks at 1612.49 cm^{-1}, 1442.75 cm^{-1}, 1091.71 cm^{-1}, 866.04 cm^{-1} indicative of C=C stretching, O-H bending, C-N stretching and C-Cl stretching respectively. The FTIR spectra of GMS showed characteristic peaks at 2914.44 cm^{-1}, 1730.15 cm^{-1} and 1176.58 cm^{-1} indicative of C-O stretching, C-H stretching and C=O stretching respectively. The FTIR spectra of physical mixture of AM and GMS showed all characteristic peaks of AM indicating absence of chemical interaction between lipid and drug. The FTIR spectra of lyophilized AM-SLNs showed absence of characteristic peaks corresponding to AM but peak corresponding to GMS was present confirming the encapsulation of drug in GMS (34).

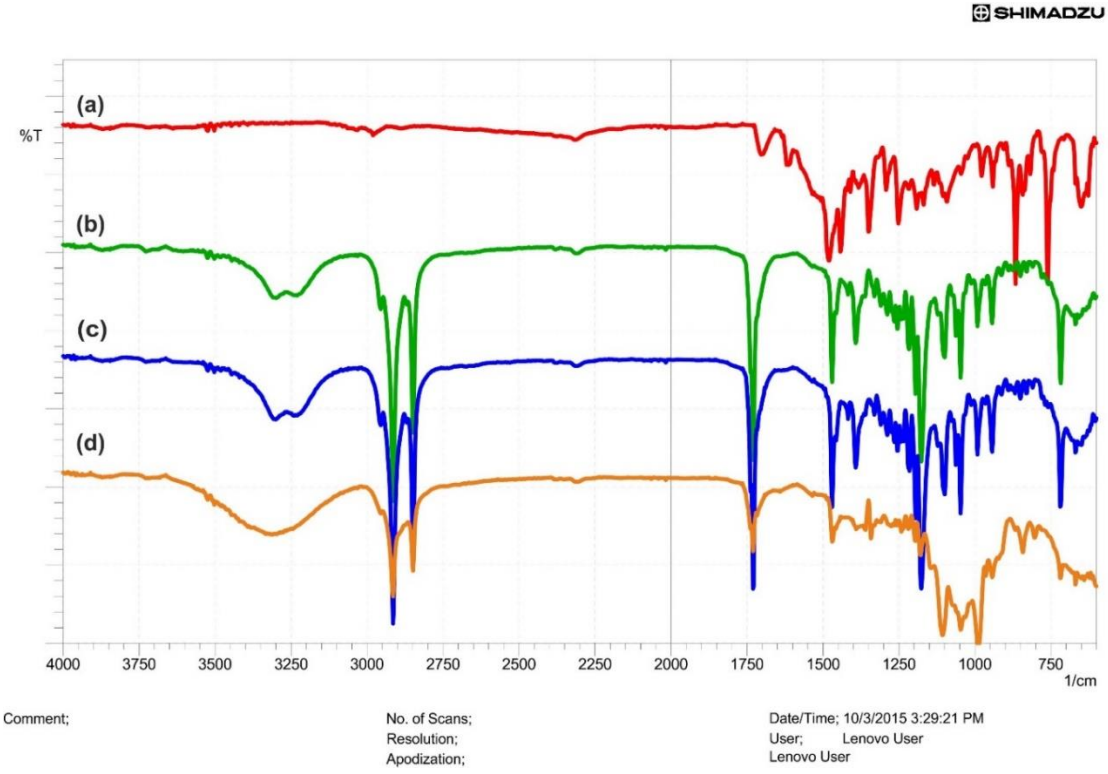

Figure 4.17: FTIR spectrum of (a) AM (b) GMS (c) Physical mixture and (d) lyophilized AM-SLNs

4.13.5 Differential Scanning Calorimetry (DSC)

The DSC thermogram of bulk AM, GMS, physical mixture of AM and GMS and lyophilized AM-SLNs are shown in figure 4.18. The DSC thermogram of AM showed sharp endothermic peak at 143.33 °C indicating its melting point and crystalline nature. The thermogram of GMS showed peak at 62.72 °C related to its melting point. The physical mixture of AM and GMS showed the melting endotherm at 62.74 °C corresponding to melting point of GMS. It showed absence of melting endotherm of drug indicating that the drug is completely solubilized in lipid. The absence of endothermic peak of AM in lyophilized AM-SLNs indicates conversion of crystalline state of drug to amorphous state. Additional peak at ~49 °C might be due to presence of surfactant (Poloxamer 188). The decrease in the peak and onset of temperature (~56 °C) of lipid can be attributed to transforming a bulk lipid into nanoparticle which reduces particle size and increase in surface area leading to a decrease in melting enthalpy (35). However, the peak at ~86 °C is due to the trehalose used as cryoprotectant in the lyophilization of SLN.

Several factors can influence the crystallinity degree, such as lyophilization and the presence of drug and surfactant. For less-ordered crystals or amorphous solids, the

melting of the substance requires much less energy than crystalline substances that need to overcome lattice forces (36). The phase transition temperature of colloidal dispersions was always much lower than the anhydrous lipid mixtures. The melting points of colloidal systems were distinctly decreased by about 3–8 °C. The melting point decrease of colloidal systems can be assigned to the colloidal dimensions of the particles in particular to their large surface to volume ratio. Nevertheless, the melting point reduction of the different formulations has no apparent relation to the particle size. In accordance with the literature reports the phase transition temperature and enthalpy of SLN formulation was significantly lower than their corresponding anhydrous physical mixture (34). In our study, phase transition temperature of SLN was lowered than anhydrous physical mixture. Therefore, lower melting enthalpy value suggest distortion in lattice arrangement in lyophilized SLN. As a result, it can be concluded that the lipid within the SLNs must be in a less ordered arrangement compared to the pure glyceryl monostearate.

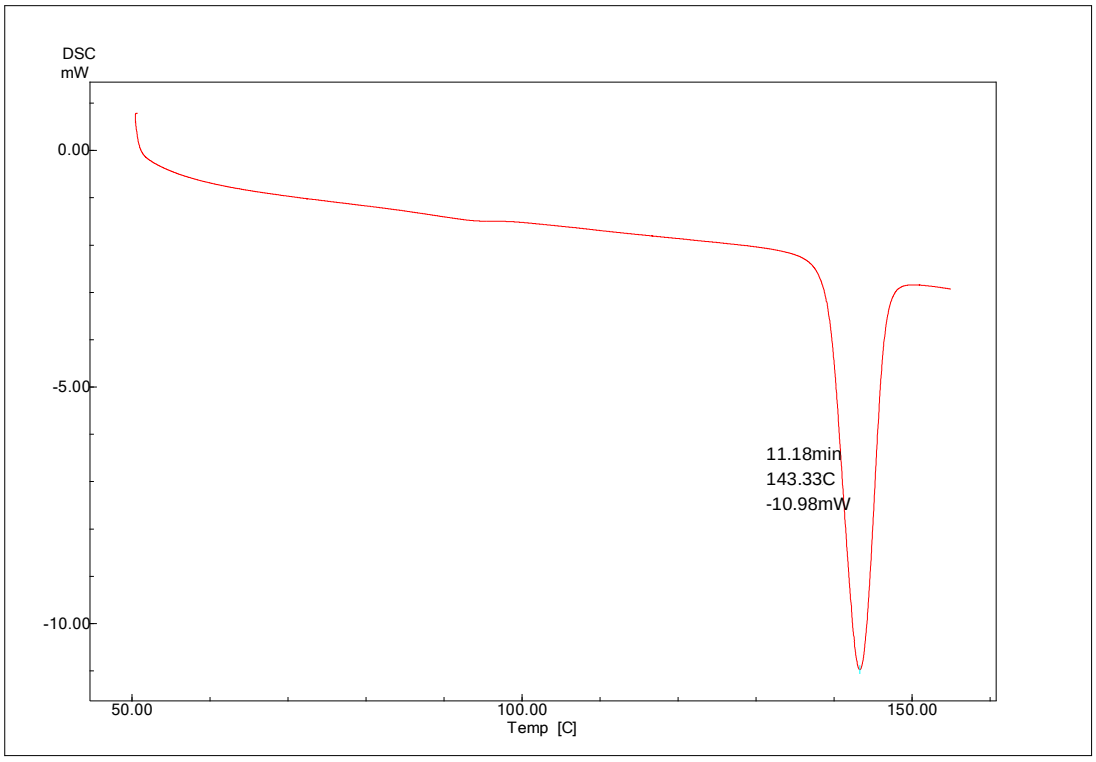

(a)

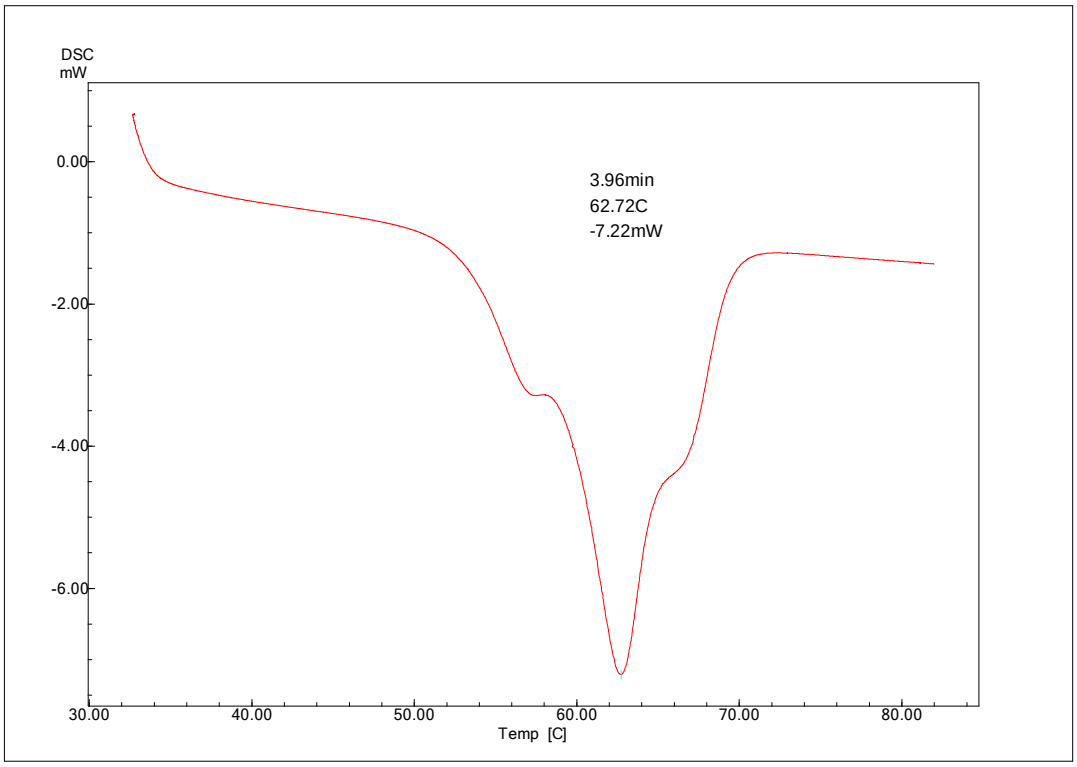
DSC
mW
0.00
-2.00
-4.00
-6.00
3.96min
62.72C
-7.22mW
30.00
40.00
50.00
60.00
70.00
80.00
Temp [C]

(b)

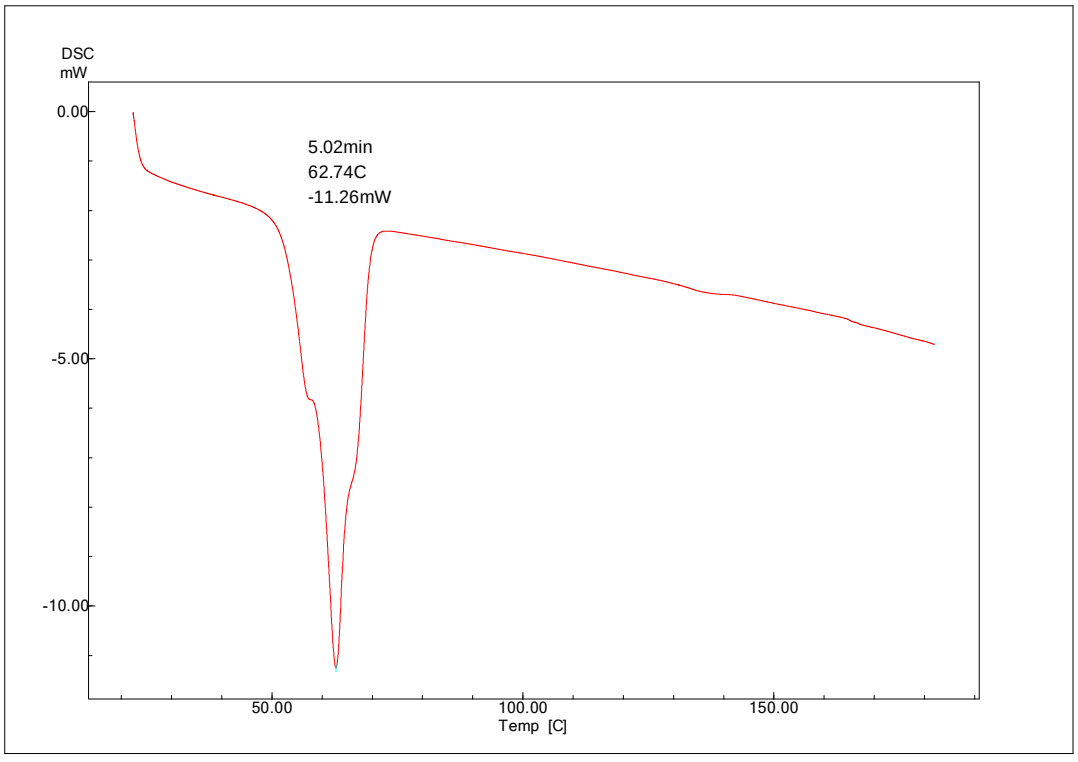
DSC
mW
0.00
-5.00
-10.00
5.02min
62.74C
-11.26mW
50.00
100.00
150.00
Temp [C]

(c)

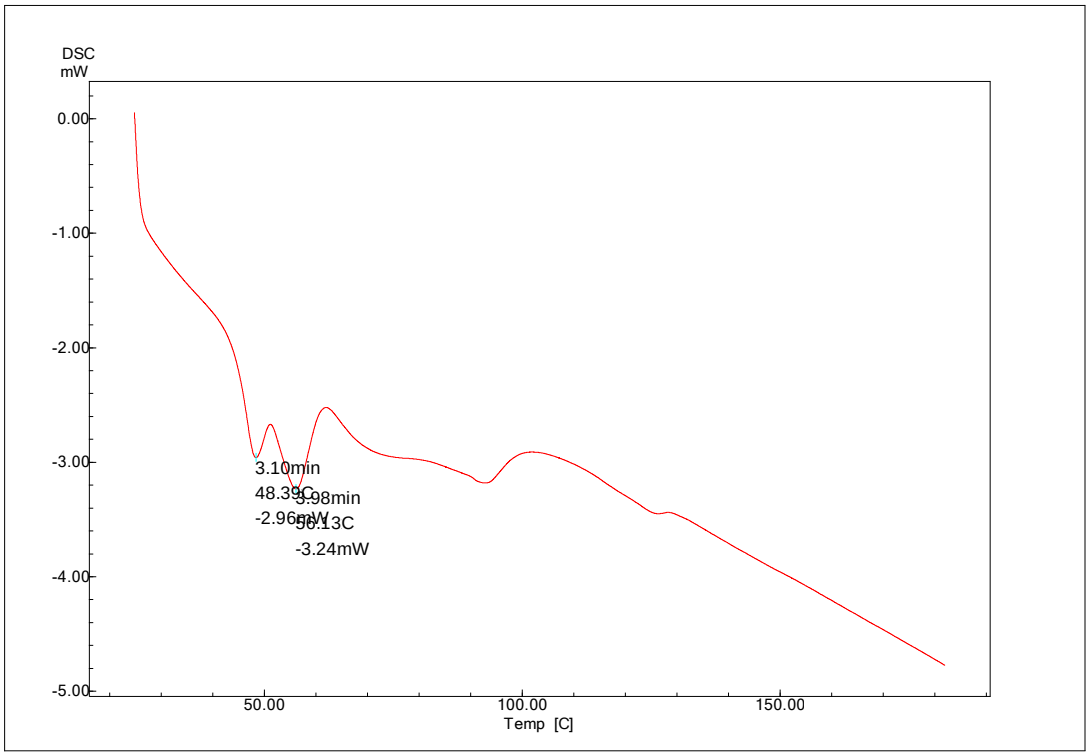

(d)

Figure 4.18: DSC thermogram of (a) AM (b) GMS (c) Physical mixture of AM and GMS (d) lyophilized AM-SLNs

4.13.6 X Ray Diffraction (XRD) study

X-ray analysis is necessary to measure crystallinity and lipid modifications which are strongly correlated with drug incorporation and release rates.

The diffractograms of bulk AM, GMS, physical mixture of AM and GMS and lyophilized AM-SLNs are shown in figure 4.19. The diffraction pattern of AM showed distinct sharp peak at 2Θ=17.8°, 18.5°, 19.6°, 22.5°, 23.6°, 29.6°, 36.2°, 39.5°, 43.5° and 48.7° indicating crystalline nature of AM. The diffraction pattern of GMS showed peak at 2Θ=19.1°, 22.9°, 29.6°, 36.4°and 39.8°. The characteristic peaks of AM could not be detected in physical mixture of drug and lipid which indicates complete solubilization of drug in the GMS. The degree of crystallinity was compared on the basis of peak intensities. The absence of typical peaks of AM in lyophilized AM-SLNs confirmed the amorphization of drug in lipid matrix. The change in crystallinity of lipid and drug is having the influence on the release of AM from SLNs. Moreover, this also indicated incorporation of AM between crystal lattice of the lipid, leading to more imperfections in the crystal and confirming that the drug

would remain entrapped in lipid matrix during the shelf life by completely solubilizing in lipid. In the preparation of SLN, AM was dissolved in GMS. This allowed homogenous dispersion of drug in the lipid. This confirmed that our method of preparation (homogenization followed by ultrasonication) and presence of surfactants prevented drug from crystallizing (35,37).

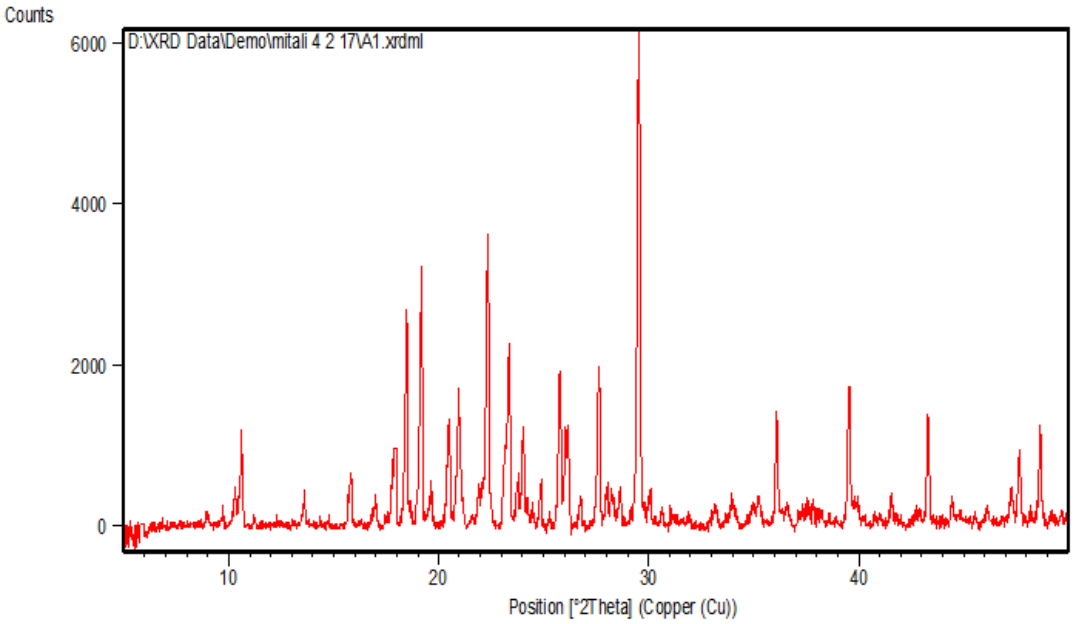

(a)

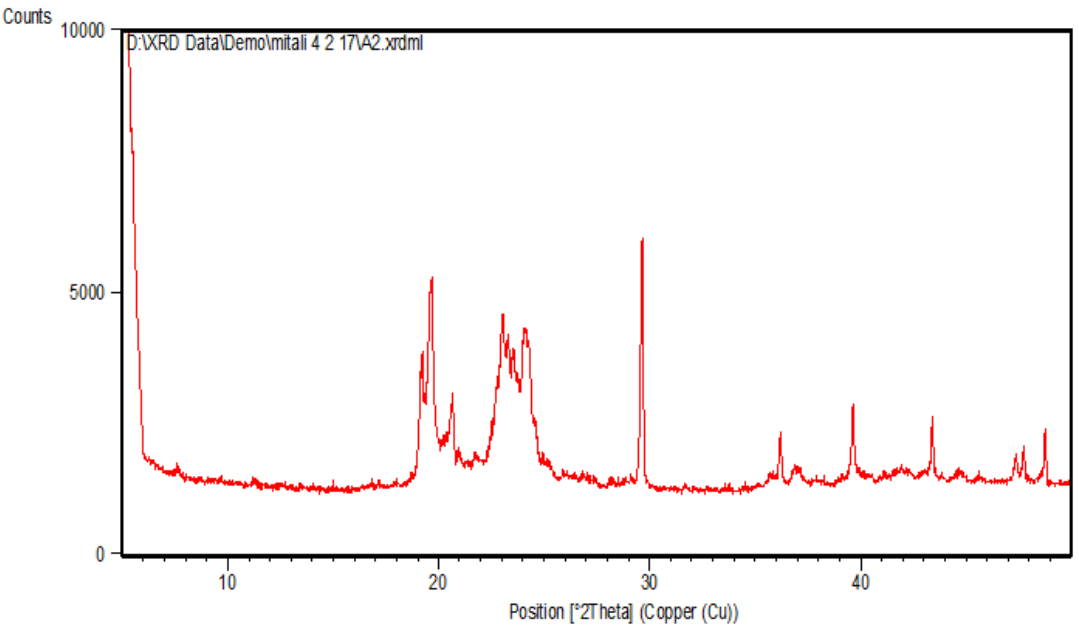

(b)

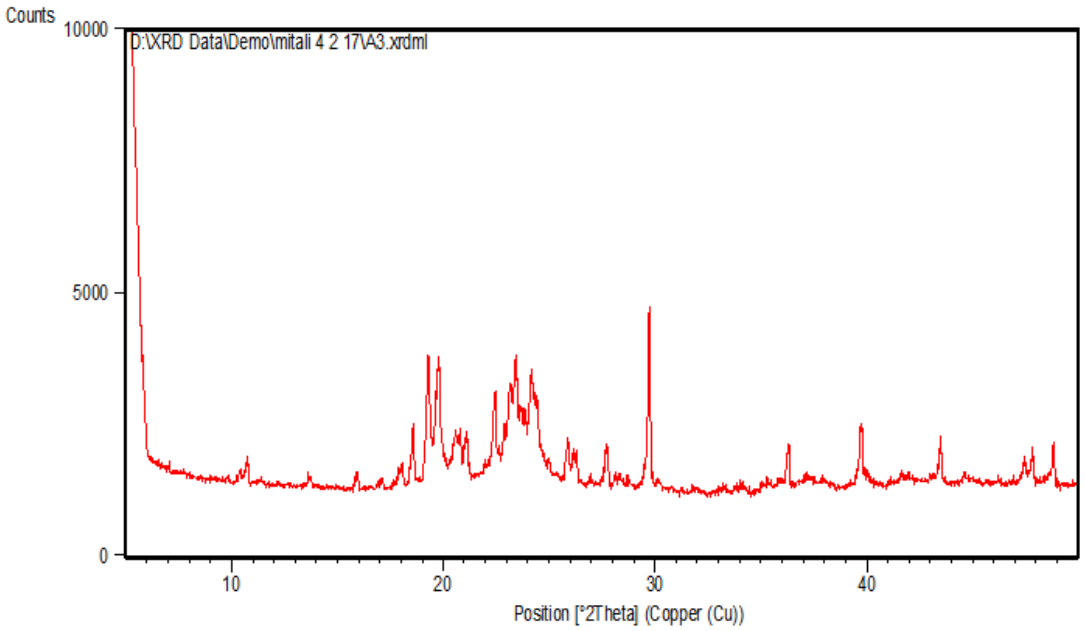

(c)

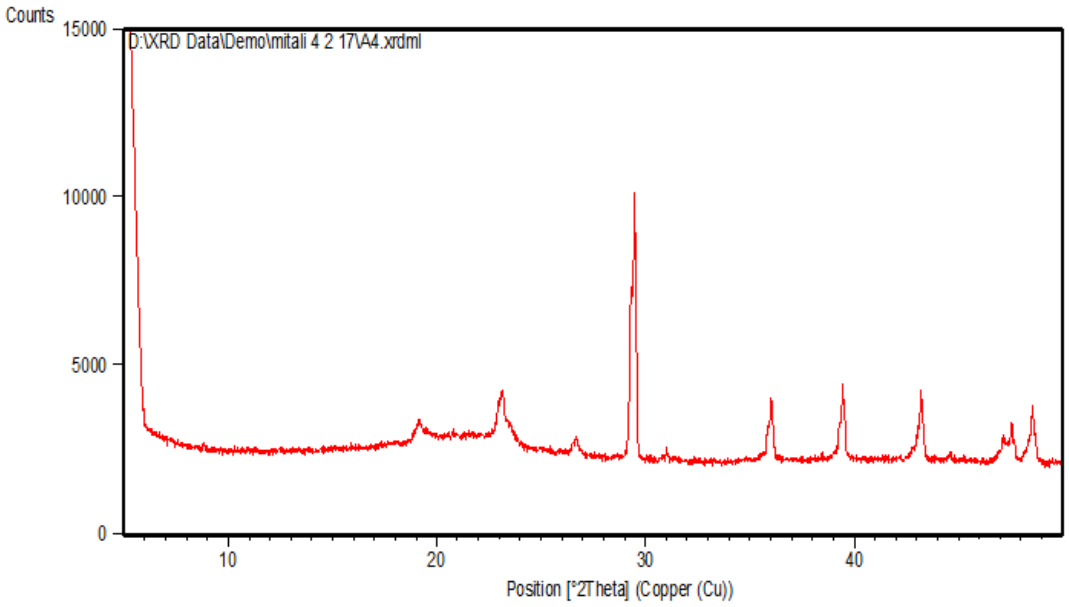

(d)

Figure 4.19 : XRD of (a) AM (b) GMS (c) physical mixture of AM and GMS (d) lyophilized AM-SLNs

4.13.8 Transmission Electron Microscopy (TEM)

The TEM image of the AM-SLNs (Figure 4.20) typically exhibit a spherical shape, and a dense lipid matrix without aggregation. The particle size observed by TEM was found to be 80-120 nm which was in accordance with the results obtained with Malvern zetasizer.

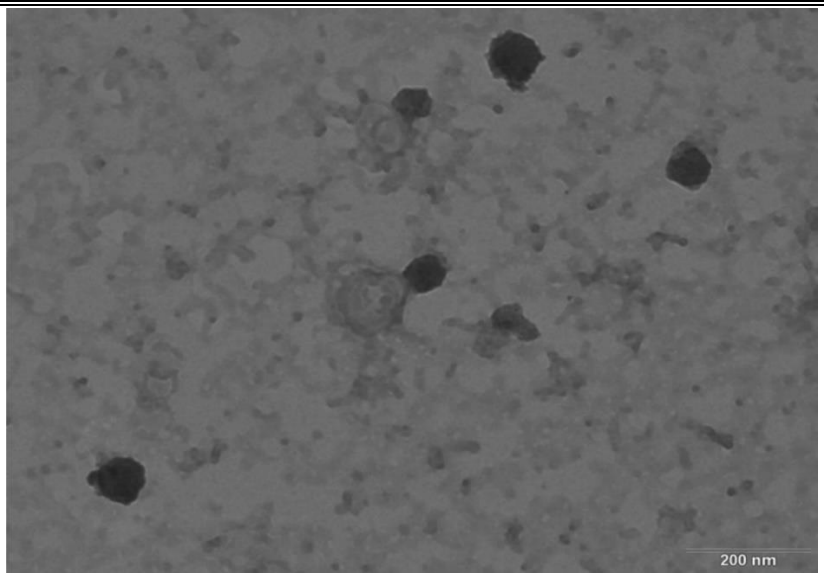

Figure 4.20: TEM image of optimized batch of AM-SLNs

4.14 IN VITRO DRUG RELEASE STUDY

In vitro drug release profile of AM-SLNs and plain drug suspension is shown in figure 4.21. The release profile of AM suspension indicated rapid diffusion of drug (89.92±3.03%) through dialysis membrane in acidic medium with subsequent release (93.42±3.26%) in phosphate buffer.

In contrast, drug release from AM loaded SLN showed only 9.23±2.72% in acidic medium indicating inclusion of AM into lipid nanoparticles significantly reduced the drug release at acidic medium. A slow and sustained release of AM (92.09±3.40%) from AM-SLNs was observed in phosphate buffer pH 6.8 at the end the 24 h indicating this phase in controlled by diffusion of drug from lipid matrix. This can be explained by slow diffusion of solubilized AM from the inner solid lipid core matrix of the SLN where it is probably entrapped in its solubilized form, to the surface of SLNs, from where it is released and passes across the dialysis membrane. During the preparation of SLNs, AM was added to the GMS (lipid) and it was found to dissolve completely in this phase. Hence, it can be said that the developed AM-SLNs followed drug-enriched core model. In this model, the drug-enriched core is surrounded by a drug free lipid shell which provides increased diffusional distance and hindering effects and hence, the drug has a controlled release profile (30). The slow release of AM from AM-SLNs suggests that AM was homogeneously dispersed in the lipid matrix.

The induction and sustained release periods can be mainly related to the drug diffusion from the core of the nanoparticle onto the surface. Moreover, it has been

reported that Poloxamer 188, a swellable, hydrophilic macromolecule, forms a hydrogel barrier and can hence control drug diffusion along with the lipid layers (39). Such sustained release of AM from AM-SLNs in phosphate buffer may result in effective treatment in vivo.

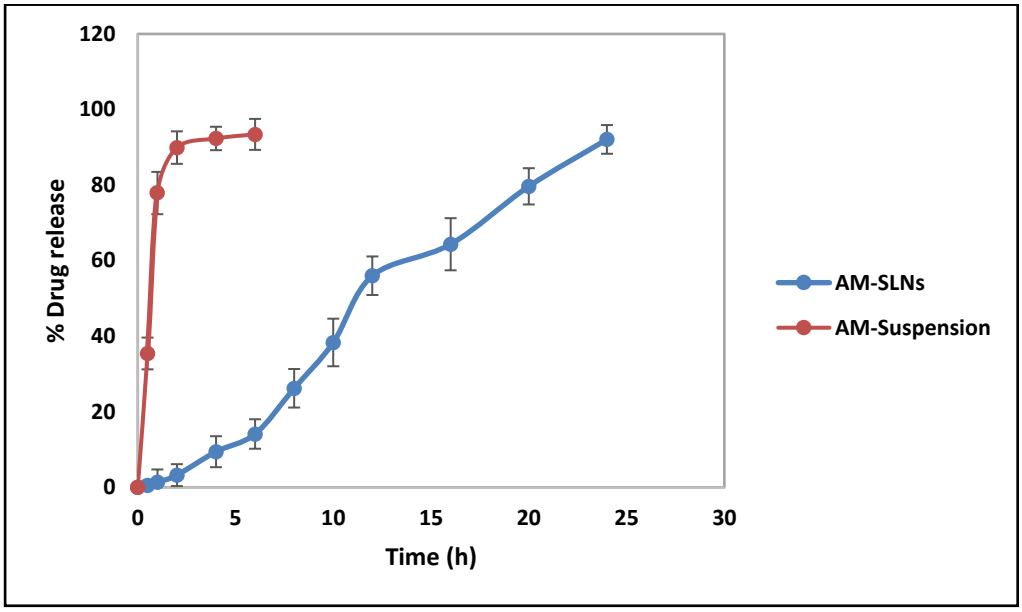

Figure 4.21: In vitro drug release profile of AM-SLNs and drug suspension

Various release models viz. zero order, first order, Korsmeyer Peppas, Hixson Crowell, Higuchi, Zero-order model and First-order were applied on the release data. Of the various release models, AM-SLN fitted well to Korsmeyer Peppas model (Table 4.22). The drug release from SLNs is usually considered as a combination of Fickian (diffusion) and non-Fickian transport of drug molecules through the lipid layers. The release exponent was found to be 0.202 indicating classical fickian drug release mechanism (38). Drug release from the AM suspension was found to be first order kinetics i.e. concentration dependent release.

Table 4.22: Correlation coefficient value of AM release kinetics

Formulation code	Correlation coefficient value (R^2)				
	Zero	First	Higuchi	Korsmeyer Peppas	Hixon-crowell
AM-SLNs	0.9727	0.9594	0.903	0.9818	0.9671
AM-suspension	0.5448	0.8643	0.7947	0.1899	0.7111

4.15 EX VIVO PERMEABILITY STUDY

The ex vivo drug release studies (Figure 4.22) in stomach and intestine were performed to simulate the gastric emptying time and to study the release pattern of drug from SLNs in gastric environment. In case of drug suspension, 87.23±1.87% of AM was diffused through stomach whereas only 1.5% AM was diffused through intestine indicating very less amount drug would be reaching to intestine and less amount of drug will be available for lymphatic uptake.

AM loaded SLNs showed only 7.23±5.54% AM was diffused from SLNs in the stomach. Subsequent diffusion of the AM through intestine was relatively slower and total 99.45±3.70% of drug was diffused at the end of 24 h indicating slow and sustained release of AM from AM-SLNs (17) indicating significant amount of AM will be carried to the intestine by incorporating into SLNs. Moreover, small particle size and presence of permeation enhancer excipient (TPGS) in the SLNs might lead to an enhanced and effective absorption of AM. Hence, it can be concluded that permeability of AM was enhanced by incorporating it in SLNs which could help in enhancing oral bioavailability of AM via lymphatic uptake.

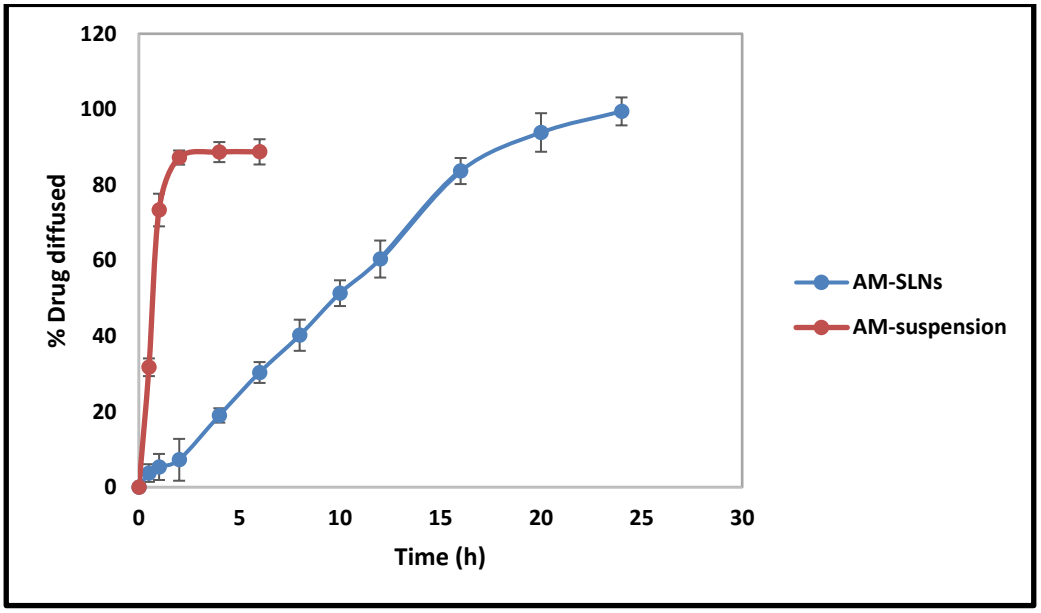

Figure 4.22 : Ex vivo drug release profile of AM-SLNs and drug suspension

4.16 STABILITY STUDY

The stability of optimized AM-SLNs was monitored for 3 months at 2-8 °C and RT in terms of particle size, zeta potential and drug content (Table 4.23). No significant change was observed in any of the assessed parameters when they were stored at refrigerated condition.

However, particle size was increased whereas zeta potential and drug content was decreased when they were stored at RT. Drug content was decreased at 30 °C because of drug expulsion from the lipid matrices at higher temperature (40). According to the DLVO theory, a system can be regarded as stable if the electrostatic repulsion dominates the attractive van der Waals forces. The particles have to overcome an energy barrier of electrostatic repulsion to approach closely and form agglomerates. If their velocity or kinetic energy is high enough they will collide. At high temperature (30°C), the kinetic energy of a system increased which dominated the attractive forces (reduced zeta potential) over repulsive forces which may lead to particle aggregation (41). Hence, recommended storage condition for better stability of AM loaded SLN is under refrigeration.

Table 4.23: Characteristics of AM-SLNs after 3-months stability studies at different conditions

Time (months)	**Refrigerated condition (2-8 °C)**			**Room temperature (30 ± 2°C/60% ± 5% RH)**		
	Particle size (nm)	**Zeta potential (mV)**	**Drug content (%)**	**Particle size (nm)**	**Zeta potential (mV)**	**Drug content (%)**
Initial	114.0±2.9	-12.9±3.5	99.1±1.2	114.0±2.9	-12.9±3.5	99.1±1.2
1 month	114.3±3.5	-12.5±4.7	99.1±2.3	124.5±5.3	-11.4±4.3	98.2±2.4
2 months	115.7±3.1	-11.8±2.9	98.5±1.5	147.8±6.2	-9.8±3.7	97.6±1.8
3 months	116.8±4.5	-11.4±4.2	98.2±2.7	173.2±4.9	-8.4±2.7	95.4±3.8

4.17 REFERENCES

1. Park S, Choo G. Hwang S, Kim M. Quality by design: screening of critical variables and formulation optimization of Eudragit E nanoparticles containing dutasteride. Arch Pharm Res. 2013;36:593-601.
2. Sawant KK, Patel MH, Patel K. Cefdinir nanosuspension for improved oral bioavailability by media milling technique: formulation, characterization and in vitro–in vivo evaluations. Drug Dev Ind Pharm. 2016;42(5):758-68.
3. Kumar S, Randhawa JK. Preparation and characterization of Paliperidone loaded solid lipid nanoparticles. Colloids Surface B. 2013;102:562-568.
4. Das S, Ng WK, Kanaujia P, Kim S, Tan R. Formulation design, preparation and physicochemical characterizations of solid lipid nanoparticles containing a hydrophobic drug: Effects of process variables. Colloids Surface B. 2011;88:483– 489.
5. Pandey A, Karande K, Sonawane R, Deshmukh P. Applying quality by design (QbD) concept for fabrication of chitosan coated nanoliposome. J Liposome Res. 2014;24(1):37-52.
6. Kumar A, Sawant K. Application of multiple regression analysis in optimization of anastrazole-loaded PLGA nanoparticles. J Microencapsul. 2013;31(2):105-114.
7. Abdelwahed W, Degobert G, Stainmesse S, Fessi H. Freeze-drying of nanoparticles: Formulation, process and storage considerations. Adv Drug Deliv Rev. 2006;58:1688–1713.
8. Geidobler R, Winter G. Controlled ice nucleation in the field of freeze-drying: Fundamentals and technology review. Eur J Pharm Biopharm. 2013;85:214–222.
9. Soares S, Fonte P, Costa A, Andrade J, Seabra V, Ferreira D, Reis S, Sarmento B. Effect of freeze-drying, cryoprotectants and storage conditions on the stability of secondary structure of insulin-loaded solid lipid nanoparticles. Int J Pharm. 2013;456(2):370-381.
10. Patel PA, Patravale VB. AmbiOnp: Solid Lipid Nanoparticles of Amphotericin B for Oral Administration. J Biomed Nanotechnol. 2011;7:632–639.

11. Paliwal R, Rai S, Vaidya B, Khatri K, Goyal A, Mishra N, Mehta A, Vyas SP. Effect of lipid core material on characteristics of solid lipid nanoparticles for oral lymphatic delivery. Nanomed Nanotech Biol and med. 2009;5:184-191.
12. Shi LL, Cao Y, Zhu XY, Cui JH, Cao QR. Optimization of process variables of zanamivir-loaded solid lipid nanoparticles and the prediction of their cellular transport in Caco-2 cell model. Int J Pharm. 2015;478(1):60-69.
13. Singh H, Jindal S, Singh M, Sharma G, Kaur IP. Nano-formulation of rifampicin with enhanced bioavailability: Development, characterization and in-vivo safety. Int J Pharm. 2015;485(1-2):138-151.
14. Dash S, Murthy PN, Nath L, Chowdhury P. Kinetic modeling on drug release from controlled Drug delivery systems. Acta Pol Pharm Drug Res. 2010;67(3):217-223.
15. Barzegar-Jalali M, Adibkia K, Valizadeh H, Shadbad MRS, Nokhodchi A, Omidi Y, Mohammadi G, Nezhadi SH, Hasan M. Kinetic Analysis of Drug Release from Nanoparticles. J Pharm Pharm Sci. 2008;11(1):167-177.
16. Bhalekar M, Upadhaya P Madgulkar A. Formulation and characterization of solid lipid nanoparticles for an anti-retroviral drug darunavir. App Nanosci. 2017;7:47–57.
17. Joshi G, Kumar A, Sawant K. Enhanced bioavailability and intestinal uptake of Gemcitabine HCl loaded PLGA nanoparticles after oral delivery. Eur J Pharm Sci. 2014;60:80-89.
18. Yasir M, Sara UVS. Solid lipid nanoparticles for nose to brain delivery of haloperidol: in vitro drug release and Pharmacokinetics evaluation. Acta Pharm Sin B. 2014;4(6):454–463.
19. Kushwaha AK, Vuddanda PR, Karunanidhi P, Singh SK, Singh S. Development and evaluation of solid lipid nanoparticles of raloxifene hydrochloride for enhanced bioavailability. BioMed Res Int. 2013:1-9.
20. Gardouh AR, Ghorab MM, Abdel-Rahman SGS. Effect of Viscosity, Method of Preparation and Homogenization Speed on Physical Characteristics of Solid Lipid Nanoparticles. ARPN J Sci Tech. 2012;2(10):996-1006.
21. Husseini GA, Pitt WG. Micelles and Nanoparticles for Ultrasonic Drug and Gene Delivery. Adv Drug Deliv Rev. 2008;60(10):1137–1152.
22. Siddiqui A, Alayoubi A, El-Malah Y, Nazzal S. Modeling the effect of sonication parameters on size and dispersion temperature of solid lipid

nanoparticles (SLNs) by response surface methodology (RSM). Pharm Dev Technol. 2013;19(3):342-346.

23. Rahman Z, Zidan AS, Habib MJ, Khan MA. Understanding the quality of protein loaded PLGA nanoparticles variability by Plackett-Burman design. Int J Pharm. 2010;389:186-194.
24. Ravi PR, Vats R, Dalal V, Murthy AN. A hybrid design to optimize preparation of lopinavir loaded solid lipid nanoparticles and comparative pharmacokinetic evaluation with marketed lopinavir/ritonavir coformulation. J Pharm Pharmacol. 2013;66:912-926.
25. Sharma N, Madan P, Lin S. Effect of process and formulation variables on the preparation of parenteral paclitaxel-loaded biodegradable polymeric nanoparticles: A co-surfactant study. Asian J Pharm Sci, 2016;11:404-416.
26. Abdel-Salam FS, Elkheshen S, Mahmoud AA, Ammar H. Diflucortolone valerate loaded solid lipid nanoparticles as a semisolid topical delivery system. Bull Fac Pharm. 2016;54:1-7.
27. Zhao S, Yang X, Garamus V, Handge U, Berengere L, Lin Zhao, Salamon G, Willumeit R, Zou A, Fan S. Mixture of nonionic/ionic surfactants for the formulation of nanostructured lipid carriers: Effect on physical properties. Langmuir. 2014;30:6920-6928.
28. Dwivedi P, Khatik R, Khandelwal K, Taneja I, Raju KSR, Wahajuddin, Sarvesh, Paliwal SK, Dwivedi AK, Mishra PR. Pharmacokinetics study of arteether loaded solid lipid nanoparticles: An improved oral bioavailability in rats. Int J Pharm. 2014;466:321–327.
29. Shah MK, Madan P, Lin S. Preparation, in vitro evaluation and statistical optimization of carvedilol-loaded solid lipid nanoparticles for lymphatic absorption via oral administration. Pharm Dev Technol. 2014;19(4):475-485.
30. Venishettya VK, Chede R, Komuravelli R, Adepu L, Sistla R, Diwan PV. Design and evaluation of polymer coated carvedilol loaded solid lipid nanoparticles to improve the oral bioavailability: A novel strategy to avoid intraduodenal administration. Colloids Surfaces B. 2012;95:1– 9.
31. Howard MD, Lu X, Jay M, Dziubla TD. Optimization of the lyophilization process for long-term stability of solid–lipid nanoparticles. Drug Dev Ind Pharm. 2012;38(10):1270–1279.

32. Subedi RK, Kanga KW, Choi HK.Preparation and characterization of solid lipid nanoparticles loaded with doxorubicin Eur J Pharm Sci. 2009;37:508–513.
33. Schwarz C, Mehnert W. Freeze-drying of drug-free and drug-loaded solid lipid nanoparticles (SLN). Int J Pharm. 1991;157:171–179.
34. Burra M, Jukanti R, Janga KY, Sunkavalli S, Velpula A, Ampati S, Jayaveera KN. Enhanced intestinal absorption and bioavailability of raloxifene hydrochloride via lyophilized solid lipid nanoparticles. Adv Powder Technol. 2013;24:393–402.
35. Carvalho SM, Noronha CM, Floriani CL, Lino RC, Rocha G, Bellettini IC, Ogliari PJ, Barreto PLM. Optimization of α-tocopherol solid lipid nanoparticles by central composite design. Ind Crops Prod. 2013;49:278-285.
36. Almeida EDP, Costa AA, Serafini MR, Rossetti FC, Marchetti JM, Sarmento VHV, Nunes RS, Valerio MEG, Araujo AA, Lira AAM. Preparation and characterization of chloroaluminum phthalocyanine-loaded solid lipid nanoparticles by thermal analysis and powder X-ray diffraction techniques. J Therm Anal Calorim. 2012;108:191–196.
37. Gande S, Kopparam M, Vobalabonia V, Vemula S. Preparation, characterization and In vitro and In vivo Evaluation of Lovastatin Solid Lipid Nanoparticles. AAPS PharmSciTec. 2007;8(1):E162–E170.
38. Silva AC, Amarala MH, Gonzalez-Mira E, Ferreira. SD Solid lipid nanoparticles (SLN) - based hydrogels as potential carriers for oral transmucosal delivery of Risperidone: Preparation and characterization studies. Colloids Surf B. 2012;93:241– 248.
39. Nabi-Meibodi M, Vatanara A, Najafabadi AR, Rouini MR, Ramezani V, Gilani K, Etemadzadeh SMH, Azadmanesh K. The effective encapsulation of a hydrophobic lipid-insoluble drug in solid lipid nanoparticles using a modified double emulsion solvent evaporation method. Colloids Surf B. 2013;112:408–414.
40. Ekambaram P, Hasan SAA. Formulation and Evaluation of Solid Lipid Nanoparticles of Ramipril. J Young Pharm. 2011;3(3):216-220.
41. Freitas C, Muller RH. Effect of light and temperature on zeta potential and physical stability in solid lipid nanoparticle (SLN™) dispersions. Int J Pharm. 1998;168:221–229.